LLM-ERM: Sample-Efficient Program Learning via LLM-Guided Search

Shivam Singhal Texas A&M University

Eran Malach Harvard University Tomaso Poggio MIT **Tomer Galanti** Texas A&M University

ABSTRACT

We seek algorithms for program learning that are both sample-efficient and computationally feasible. Classical results show that targets admitting short program descriptions (e.g., with short "python code") can be learned with a "small" number of examples (scaling with the size of the code) via length-first program enumeration, but the search is exponential in description length. Consequently, Gradient-based training avoids this cost yet can require exponentially many samples on certain short-program families.

To address this gap, we introduce LLM-ERM, a propose-and-verify framework that replaces exhaustive enumeration with an LLM-guided search over candidate programs while retaining ERM-style selection on held-out data. Specifically, we draw k candidates with a pretrained reasoning-augmented LLM, compile and check each on the data, and return the best verified hypothesis, with no feedback, adaptivity, or gradients. Theoretically, we show that coordinate-wise online mini-batch SGD requires many samples to learn certain short programs. Empirically, LLM-ERM solves tasks such as parity variants, pattern matching, and primality testing with as few as 200 samples, while SGD-trained transformers overfit even with 100,000 samples. These results indicate that language-guided program synthesis recovers much of the statistical efficiency of finite-class ERM while remaining computationally tractable, offering a practical route to learning succinct hypotheses beyond the reach of gradient-based training.

1 Introduction

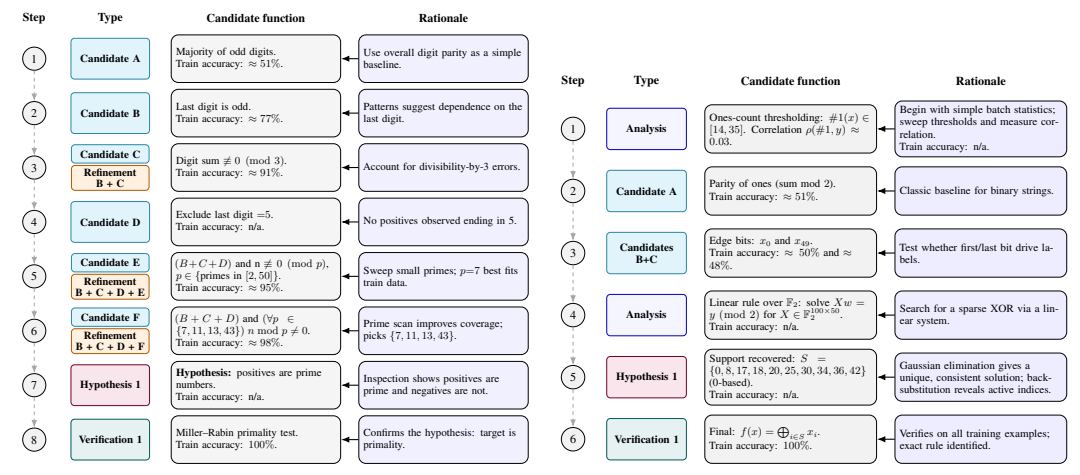
At its core, machine learning seeks algorithms that uncover structure in data: given input–output examples, the goal is to recover an unknown function that generalizes to unseen inputs. Classical learning theory provides conditions under which this is possible. In particular, when the target lies in a finite hypothesis class, empirical risk minimization (ERM) requires only a modest number of samples—scaling logarithmically with the class size (Valiant, 1984; Vapnik, 1998). For example, if the target can be expressed as a short program of length L over an alphabet Σ , then $\mathcal{O}(L \log |\Sigma|)$ samples suffice.

The challenge lies in computation. Exhaustive program enumeration guarantees that we will eventually find the needle, but only by sifting through an exponentially large haystack of candidate programs. Concretely, if the target program has length L over an alphabet Σ , then the number of candidate strings of length at most L is $|\mathcal{L}_{\leq L}| = \sum_{\ell=1}^L |\Sigma|^\ell = \Theta(|\Sigma|^L)$. Even when verifying each candidate requires only linear time in the sample size m, the total runtime scales as $\Theta(m |\Sigma|^L)$. In practice, this brute-force search becomes infeasible even for modest L (e.g., L=20 with $|\Sigma|$ =10 already yields 10^{20} candidates).

Modern deep learning flips this trade-off. Rather than searching the haystack directly, a common approach is to train neural networks via stochastic gradient descent (SGD) (Robbins and Monro, 1951; Bottou, 2010). This is computationally efficient: one typically fits the data in a total runtime of O(mE), where



Figure 2: Trade-offs between sample and computational efficiency in program learning. The proposed method (LLM-ERM) lies in the intersection.



- (a) **Reasoning trace for learning primality.** The model starts with digit heuristics, eliminates small-prime multiples, and converges to the Miller–Rabin test.
- (b) **Reasoning trace for learning a Random 10-Parity function.** The model starts from simple heuristics, shifts to linear algebra over F2, and ultimately identifies the exact XOR rule over 10 specific indices.

Figure 1: Side-by-side comparison of reasoning traces for two distinct learning tasks. Rules were proposed by GPT-5-Thinking in a single run until convergence. Train accuracy values shown are those the model decided to compute and explicitly include in its reasoning trace. In each subfigure the two columns, **Left:** sequence of proposed rules and **Right:** rationale for each proposal.

E is a modest number of epochs. However, in the statistical query (SQ) framework (Kearns, 1998), algorithms such as online SGD oftentimes require exponentially many samples on certain high–SQ-dimension families—such as parity or cryptographic-like functions—even though these targets admit succinct program representations. In short, gradient-based methods fail not because the target is deeply hidden, but because their search procedure is poorly matched to the structure of the hypothesis space.

Can we design learning algorithms that combine the sample efficiency of finite-class program search with the computational efficiency of modern optimization methods?

Contributions. We revisit program learning through the lens of LLMs and ask whether pretrained reasoning can bridge the gap between statistical and computational efficiency. Our contributions are:

- Theory: SGD lower bounds via SQ. Using tools from (Feldman et al., 2018), we rigorously show how statistical-query (SQ) hardness translates into *iteration* complexity for coordinate-wise mini-batch (online) SGD. For high SQ-dimension families (e.g., parity), we prove lower bounds where—even if a short correct program exists—gradient-based learners may need exponentially many samples/iterations to reach nontrivial error. In contrast, in the realizable short-program regime, finite-class ERM over programs of length L achieves sample complexity $\mathcal{O}(\frac{1}{\epsilon}(L \log |\Sigma| + \log(\frac{L}{\delta})))$, independent of input dimension, but computationally exponential in L.
- Algorithm: propose-verify LLM-ERM. We introduce an LLM-guided synthesis procedure that maintains a finite pool of candidate programs and selects among them via empirical risk minimization on held-out data. LLM feedback proposes discrete edits that bias search toward promising regions of program space. The outer loop is gradient-free and non-adaptive w.r.t. validation (early stopping below a threshold), preserving ERM-style generalization while dramatically shrinking the search relative to naive enumeration.
- Empirics: sample efficiency and cross-dimension generalization. Across a suite of algorithmic tasks (e.g., parity variants (Full/First-Half/Random-k), pattern matching, palindromes, Dyck-2, primality testing, cellular-automata parity, and SHA-256 parity), LLM-ERM typically recovers the *exact* target rule from only 200 labeled examples and generalizes strongly (Figs. 5, 11; Tab. 1). For many cases (e.g., parities, IsPrime), the synthesized programs are *dimension-invariant*, yielding

effectively unbounded test accuracy when evaluated beyond the training length (see Tab. 1). On palindromes and Dyck-2, LLM-ERM discovers high-accuracy but not always exact parsers. In sharp contrast, SGD-trained transformers (e.g., Qwen3-1.7B) fit the training data yet collapse to chance on non-local/recursive tasks, and even scaling to 100k examples fails to fix generalization for Random 10-Parity, Cellular Automata Parity, and digit-restricted IsPrime (Fig. 6). This failure also appears when adapting pre-trained models, as both fine-tuning and in-context learning with LLMs result in near-chance test performance on the same non-local tasks (Figs. 8 and 9). Finally, both approaches remain near chance on SHA-256 parity, highlighting a high-bar for learning. These trends are robust across model architecture, learning rate, and batch size.

• Interpretability: the final hypothesis and the learning process are interpretable by construction. The output is executable, human-readable code accompanied by an auditable reasoning trace (Figs. 1, 18 and 19). This makes both the learned function and the learning process interpretable. One can inspect intermediate candidates, understand why they were proposed, and validate the final rule mechanistically (e.g., Miller–Rabin for IsPrime, XOR over specific indices for k-parities), enabling counterfactual edits and dimension-transfer tests.

1.1 RELATED WORK

PAC learning, Occam's razor and short programs. We follow the classical generalization theory, where finite-class ERM has sample complexity $\mathcal{O}(\log |\mathcal{H}|)$ (Valiant, 1984; Vapnik and Chervonenkis, 1971; Vapnik, 1998). The "short program" view instantiates Occam/MDL: a hypothesis encodable in L symbols over alphabet Σ admits bounds of order $\mathcal{O}(L \log |\Sigma|)$, up to confidence terms (Blumer et al., 1987; Barron and Cover, 1991; Barron et al., 1998; Rissanen, 1989; McAllester, 1998). The length-first search (Alg. 2) realizes this ERM guarantee but incurs exponential time in description length, reflecting the classic universal-search trade-off (Levin, 1973; Solomonoff, 1964).

Statistical query (SQ) learning and hardness of learning. The SQ framework and its refinements (Kearns, 1998; Blum et al., 1994; Feldman, 2017; Reyzin, 2020) yield lower bounds for many concept classes. Parity and related families have large SQ dimension under the uniform distribution, so any SQ learner needs exponentially many (tolerant) queries to achieve nontrivial correlation (Blum et al., 1994; Feldman et al., 2017; Klivans and Sherstov, 2007; Klivans and Kothari, 2014; Giapitzakis et al., 2025). Intuitively, mini-batch SGD is itself approximately an SQ algorithm: each update averages a bounded statistic over samples (Feldman et al., 2017; 2018; Abbe et al., 2021; Barak et al., 2022). Hence, SQ lower bounds transfer directly to SGD, making its iteration complexity grow with the SQ dimension—exponentially for parities and pseudorandom families under the uniform distribution. Our analysis formalizes this connection, showing how SQ hardness induces exponential sample requirements for gradient-based methods.

Gradient-based training on algorithmic reasoning. Beyond worst-case bounds, a long line of work studies when expressive neural families are actually *trainable* with SGD, separating representational power from optimization and sample efficiency (Yehudai and Shamir, 2019; Daniely, 2017). Empirically, SGD-trained neural networks often struggle on parity-like or compositional algorithmic tasks without strong inductive bias or very large data, even when the target is compactly describable (Shalev-Shwartz et al., 2017; Safran and Shamir, 2018; Daniely and Malach, 2020; Barak et al., 2022). The "grokking" phenomenon—delayed generalization after long training on small algorithmic datasets—further highlights the mismatch between the statistical optimum and what SGD discovers (Power et al., 2022). These observations motivate alternatives that retain finite-class guarantees while improving practical search efficiency.

LLM-guided optimization and evolutionary feedback. Since the advent of LLMs, researchers have explored ways to elicit task solutions directly via prompting. One line of work is *in-context learning* (ICL), where demonstrations—often with chain-of-thought—induce task procedures without parameter updates (Brown et al., 2020; Min et al., 2022; Wei et al., 2022). Its learning capabilities have been analyzed in a series of papers (Von Oswald et al., 2023; Akyürek et al., 2023; Shen et al., 2024; de Wynter, 2025). Beyond ICL, natural-language or symbolic feedback enables iterative propose—critique—revise loops (e.g., Self-Refine, Reflexion) and even *textual gradients* that treat feedback as a search direction in discrete spaces (Madaan et al., 2023; Shinn et al., 2023; Yuksekgonul et al., 2024). In parallel, evolutionary and neuro-symbolic approaches (SOAR, AlphaEvolve, LEGO) use LLMs to propose edits or modular building blocks, refined via mutation—selection (Pourcel et al., 2025; Novikov et al., 2025; DeepMind, 2025; Bhansali et al., 2024). Within program synthesis, LLMs

have been used to generate patches, tests, and rationales that guide iterative repair and verification (Chen et al., 2024; Wang et al., 2024; Hu et al., 2025).

2 THEORETICAL ANALYSIS

2.1 PROBLEM SETUP

We study inductive program synthesis ("program learning"): the target is a binary function $y: \mathcal{X} \to \{\pm 1\}$ implemented by a short program in a fixed language, and the learner receives i.i.d. examples $S = \{(x_i, y(x_i))\}_{i=1}^m$ with $x_i \sim D$. Throughout, we assume the realizable setting, i.e., $y \in \mathcal{L}$, where \mathcal{L} is the class of total functions computed by programs in the language (formalized below).

Language and semantics. Fix a finite alphabet Σ and a programming language $\mathcal{L} \subseteq \Sigma^*$. Each string $u \in \mathcal{L}$ has semantics $\llbracket u \rrbracket : \mathcal{X} \to \{\pm 1\}$, a (possibly partial) function that may fail to compile or fail to halt. We write $\llbracket u \rrbracket (x) = \bot$ when u does not produce an output on x. Let $\mathcal{C} := \{f : \mathcal{X} \to \{\pm 1\} : \exists u \in \mathcal{L} \text{ s.t. } \llbracket u \rrbracket \text{ is total and } \llbracket u \rrbracket = f \}$. We denote the length of u by |u| (in symbols over Σ) and write $\mathcal{L}_{\ell} := \{u \in \mathcal{L} : |u| = \ell\}$. A program is considered total if it defines an output for every input—i.e., it never fails to compile and halts on all $x \in \mathcal{X}$, returning a label in $\{\pm 1\}$.

Data model and objective. The learner observes a sample $S = \{(x_i, y_i)\}_{i=1}^m$ with $x_i \overset{\text{i.i.d.}}{\sim} D$ and $y_i = y(x_i)$. For a hypothesis $h: \mathcal{X} \to \{\pm 1\}$, define population error $\text{err}_D(h) := \Pr_{x \sim D}[h(x) \neq y(x)]$ and empirical error $\text{err}_S(h) := \frac{1}{m} \sum_{i=1}^m \mathbf{1}\{h(x_i) \neq y_i\}$. The goal is to output a program $u \in \mathcal{L}$ whose total semantics $\llbracket u \rrbracket$ attains small err_D .

Computational model. When executing a candidate program u on input x, we allow a time budget $T \in \mathbb{N}$ per call; if u fails to compile or does not halt within time T, we treat the outcome as \bot and reject u as a hypothesis. This makes search procedures well-defined even when $\llbracket u \rrbracket$ is partial.

Short-program regime. We will frequently analyze the *short-program* subclass $\mathcal{H}_{\ell} := \{ \llbracket u \rrbracket : u \in \mathcal{L}_{\ell}, \llbracket u \rrbracket \text{ total} \}$, where $\mathcal{H} = \bigcup_{\ell \geq 1} \mathcal{H}_{\ell}$ and compare (i) explicit search over \mathcal{H}_{ℓ} (finite-class ERM) to (ii) gradient-based learners h_{θ} drawn from a proxy hypothesis family $\{h_{\theta} : \theta \in \Theta\}$.

2.2 PROGRAM ENUMERATION

To study the sample complexity of program learning, we frame the problem in the *Probably Approximately Correct* (PAC) paradigm (Valiant, 1984; Vapnik and Chervonenkis, 1971; Vapnik, 1998). The goal is to learn a target function $y: \mathcal{X} \to \{\pm 1\}$ from labeled examples drawn from an unknown distribution. A learning algorithm \mathcal{A} receives a sample S and a hypothesis class \mathcal{H} (e.g., all programs in \mathcal{L} or a family of neural networks), and selects $h \in \mathcal{H}$ to minimize the generalization error $\text{err}_D(h)$.

A central question in learning theory is how to design the algorithm \mathcal{A} and the hypothesis class \mathcal{H} so that the required sample size m depends favorably on the accuracy ε and confidence δ . By classical PAC learning results (Valiant, 1984) (see also Cor. 2.3 of (Shalev-Shwartz and Ben-David, 2014)), for the program-learning setting we obtain the following guarantee:

Proposition 1. Suppose we wish to learn a target function $y: \mathcal{X} \to \{\pm 1\}$ that can be implemented as a program of length L in a programming language \mathcal{L} . Let \mathcal{L}_{ℓ} denote the set of programs of length ℓ in \mathcal{L} , and let $S = \{(x_i, y(x_i))\}_{i=1}^m$ be m training examples drawn i.i.d. from a distribution D over $\mathcal{X} \times \{\pm 1\}$. Then, with probability at least $1 - \delta$ over the draw of S, length-first program enumeration (Alg. 2) outputs a program $h \in \mathcal{L}$ that is consistent with S and satisfies $\operatorname{err}_D(h) \leq \frac{1}{m}[L\log|\Sigma| + \log(\frac{2L^2}{\delta})]$.

This result demonstrates that if the target function can be expressed as a short program (i.e., if L is small), then only a modest number of samples are required to learn it, regardless of the dimensionality of the input space. Thus, program enumeration (Alg. 2) is highly *sample efficient*. However, it remains computationally infeasible: the runtime grows exponentially in L. This tradeoff between sample efficiency and computational efficiency motivates our subsequent analysis.

2.3 GRADIENT-BASED OPTIMIZATION

To address this, deep learning replaces enumeration over the discrete program set \mathcal{L} with training a neural network. We posit a parametric class $\mathcal{H} = \{h_{\theta} : \theta \in \Theta\} \neq \mathcal{L}$ (e.g., a neural network with learnable parameters θ) and use gradient-based optimization to fit $h_{\theta} \in \mathcal{H}$ to data. This is typically faster than enumerating exponentially many programs, but it does not guarantee sample complexity comparable to finite-class ERM.

2.3.1 COORDINATE MINI-BATCH SGD THROUGH THE LENS OF STATISTICAL QUERIES

Next, we analyze gradient-based optimization in the *statistical query* (SQ) framework (Kearns, 1998). An SQ learner interacts with a τ -tolerant oracle: given a bounded query function $\phi: \mathcal{X} \times \{\pm 1\} \rightarrow [-1,1]$, the oracle returns $\tilde{v} = \mathbb{E}_{(x,y) \sim D}[\phi(x,y)] + \xi$, where $|\xi| \leq \tau$, with arbitrarily ξ chosen.

In practice, queries are often answered by empirical averages over fresh i.i.d. batches, modeled by the 1-STAT and VSTAT oracles (Feldman et al., 2017). A 1-STAT returns g(x,y) for a fresh $(x,y)\sim D$, while VSTAT(t) returns $\mathbb{E}_D[g]\pm \tilde{O}(1/\sqrt{t})$. The two are equivalent up to polynomial overheads (Feldman et al., 2018, Thm. B.4).

The complexity of a concept class in this framework is captured by its *statistical query dimension*: **Definition 1** (Statistical Query Dimension (Blum et al., 1994)). For a concept class $C \subseteq \{-1, +1\}^{\mathcal{X}}$ and distribution D over \mathcal{X} , the SQ dimension $SQ\text{-DIM}_D(\mathcal{C})$ is the largest integer d for which there exist $f_1, \ldots, f_d \in \mathcal{C}$ such that $|\mathbb{E}_{x \sim D}[f_i(x)f_j(x)]| \leq 1/d$ for all $i \neq j$.

By a standard energy argument (Blum et al., 1994), if $SQ\text{-}DIM_D(\mathcal{C}) = d$, then any (stochastic) SQ learner needs $\Omega(d\epsilon^2)$ queries to reach error $\leq 1/2 - \epsilon$; see also (Reyzin, 2020, Thm. 12).

Coordinate mini-batch SGD as a stochastic SQ learner. Intuitively, online SGD resembles an SQ learner because each mini-batch update is an empirical average of a bounded query over B fresh samples. To formalize this idea, a standard approach injects independent noise in each update so that interactions with the data reduce to tolerant expectations (e.g. (Abbe et al., 2021; Barak et al., 2022)). An alternative approach is to consider *coordinate* mini-batch SGD: at iteration t, the chosen coordinate gradient is exactly a 1-STAT query averaged over B fresh samples. By the standard simulation theorem (Feldman et al., 2018, Thm. B.4), T iterations with batch size B can be simulated using $\tilde{O}(TB)$ queries to a VSTAT oracle.

Formally, let D be a distribution over $z=(x,y), \Theta\subseteq\mathbb{R}^d$ a parameter domain, $\mathcal{H}=\{h_\theta:\theta\in\Theta\}$ a hypothesis class, and $\ell(h_\theta,(x,y))$ a per-example loss with gradient $\partial\ell(h_\theta,(x,y))$. We assume per-example coordinate gradients are uniformly bounded: there exists G>0 such that $\left|\partial_j\ell(h_\theta,(x,y))\right|\leq G$ for all $\theta,j,(x,y)$; this can be ensured, for example, by bounded inputs and weights in standard neural networks, or by explicit gradient clipping. Coordinate online mini-batch SGD proceeds as follows: at round t, draw a fresh mini-batch $\{(x_{t,b},y_{t,b})\}_{b=1}^B\sim D^B$, choose a coordinate j_t independent of this batch (but \mathcal{F}_{t-1} -measurable, i.e., possibly dependent on all past information \mathcal{F}_{t-1}), set $\hat{g}_{t,j_t}=\frac{1}{B}\sum_{b=1}^B\partial_{j_t}\ell(h_{\theta_t},(x_{t,b},y_{t,b}))$, and update $\theta_{t+1}=\theta_t-\eta_t\,\hat{g}_{t,j_t}\,e_{j_t}$, where e_{j_t} is the j_t -th standard basis vector.

With the boundedness assumption, each round is the average of a bounded per-example statistic (a 1-STAT query), yielding the $\tilde{\mathcal{O}}(TB)$ simulation to VSTAT, which we use to derive iteration (hence sample) lower bounds for error below $1/2-\epsilon$. Combining this observation with the SQ-dimension lower bound yields:

Proposition 2 (Lower bound for SGD). Let \mathcal{C} be a class with $\mathrm{SQ\text{-}DIM}_D(\mathcal{C}) = d$. Consider coordinate mini-batch SGD with batch size B run for T iterations. Fix $\epsilon \in (0,1/2)$. If the algorithm outputs a hypothesis of error at most $1/2 - \epsilon$ with probability at least 2/3, then $T \geq \Omega\left(\frac{d}{B^{3/2}}\right)$.

For example, for the nontrivial parity class $\mathcal{C}_{\mathrm{par}}=\{f_s(x)=(-1)^{\langle s,x\rangle}:s\in\{0,1\}^n\}$ under the uniform distribution on $\{0,1\}^n$, we have $\mathrm{SQ}\text{-DIM}_D(\mathcal{C}_{\mathrm{par}})=2^n$. In particular, $T=\Omega\left((2^n\epsilon^2)/B^{3/2}\right)$. Thus, even when short program descriptions exist for high SQ-dimension classes, gradient-based learners such as SGD are inherently sample-inefficient: their query complexity grows exponentially with n for parity and related tasks. Full proofs, including the formal reduction from SGD to 1-STAT to VSTAT, are deferred to App. B.1.



Figure 3: An illustration of LLM-ERM. A prompt from $S_{\rm tr}$ seeds the LLM to propose candidates, which are evaluated on train and validation sets. We track the lowest validation error and stop early when it drops below θ , or otherwise after k iterations.

Algorithm 1 LLM-ERM: k-try LLM-guided search with validation

```
Require: S_{\rm tr}, S_{\rm val}; attempts k; prompt \Pi; decoding (\tau, M); threshold \theta; optional batch b
Ensure: Program u^* with hypothesis h^* = [\![u^*]\!] minimizing validation error
 1: Build query \Pi(S_{tr}); initialize err* \leftarrow 1, u^* \leftarrow \bot, h^* \leftarrow \bot, \mathcal{U} \leftarrow \emptyset
 2: for t = 1 to k do
         Query LLM with \Pi(S_{\mathrm{tr}}) (temp. \tau, max tokens M) for up to b candidates
 3:
 4:
         for each u in candidates with u \notin \mathcal{U} do
 5:
            \mathcal{U} \leftarrow \mathcal{U} \cup \{u\}; compile u; let h = \llbracket u \rrbracket
 6:
            if h undefined on some x \in S_{\mathrm{tr}} \cup S_{\mathrm{val}} then
 7:
                continue
                                                                                             {skip non-total/invalid candidates}
            end if
 8:
 9:
            Compute err_{tr}(h) and err_{val}(h)
10:
            if err_{val}(h) < err^* then
                 (\operatorname{err}^{\star}, u^{\star}, h^{\star}) \leftarrow (\operatorname{err}_{\operatorname{val}}(h), u, h)
11:
                if err^* \leq \theta then
12:
13:
                    return (u^{\star}, h^{\star})
                                                                                                           {early stop on threshold}
14:
                end if
15:
            end if
         end for
16:
17: end for
18: return (u^{\star}, h^{\star})
                                                                                           {best-by-validation if no early stop}
```

Remark 1 (Sample and runtime complexity tradeoff). Under the uniform distribution on $\{0,1\}^n$, the full parity and the k-parity concept classes admit short programs of lengths $L = \Theta(1)$ and $L = \Theta(k \log n)$, respectively. By Prop. 1, simple program enumeration attains error $\leq \varepsilon$ with $m = \mathcal{O}(1/\varepsilon)$ samples for full parity and $m = \mathcal{O}(k \log n/\varepsilon)$ samples for k-parity. Its runtime is dominated by scanning all programs of length $\leq L$ over an alphabet Σ , so time(enum) $= \mathcal{O}(m |\Sigma|^L)$.

By contrast, in the Statistical Query (SQ) model, the SQ-dimension of full parity is 2^n , while for k-parities it is $\sum_{i=0}^k \binom{n}{i} = \Theta(n^k)$ (for constant k). Consequently, any SQ learner with tolerance at least 1/poly(n)—including mini-batch SGD with polynomial batch sizes—requires $2^{\Omega(n)}$ samples for full parity and $n^{\Omega(k)}$ samples for k-parity to reach error $<\frac{1}{2}-\gamma$. Its runtime, on the other hand, satisfies time(SGD) = $\mathcal{O}(m \times (cost\ per\ gradient) \times (\#\ epochs))$, which is per example/epoch O(1) with respect to L when the model/gradient cost does not scale with the program length L.

In short: enumeration trades low sample for time exponential in L, whereas SGD trades cheap per-example computation for large sample.

3 METHOD

While brute-force program enumeration has good sample complexity, its runtime grows exponentially with program length, making it impractical even for modest tasks. Moreover, exhaustive search is *data-agnostic*: it enumerates programs in order of length, checking each against the data without exploiting structure. By contrast, our approach (Alg. 1) leverages LLMs with internal reasoning (e.g., GPT-5), which can apply algorithmic heuristics when constructing candidates—for example,

LLM Prompt

Problem Statement: Given a sequence of input vectors (binary, length {sequence_dimension}) and their corresponding scalar binary outputs ('0' or '1'), find a concise Python function f(x) that accurately approximates the underlying relationship. The function should not be a trainable model, but a direct logical or mathematical representation of the target function.

Data Examples:

```
000111101011110010100101001100 -> 1
... 011011010111000010010101001000 -> 1
You must output ONLY a single JSON object: {"code": "<python function>"}
```

Figure 4: Prompt used in our LLM-ERM procedure. We run $\mathtt{GPT-5}$ with this prompt for up to k independent iterations, each returning only Python code for a candidate target function.

simulating the Blum-Kalai-Wasserman algorithm (Blum et al., 2003), using pattern matching, or refining proposals iteratively as performance signals develop. This adaptive search, guided by data, is the key source of efficiency of our method.

Given a labeled set of samples, we prompt the LLM to generate candidate functions (Step 3 of Alg. 1). Over k iterations we collect a pool of candidates (Step 5), verify them against training and validation examples (Step 9), and select the best on the validation set with early stopping when the threshold is met (Steps 11-13). This preserves the "search-and-verify" structure of Alg. 2 but replaces exhaustive enumeration with an adaptive, LLM-guided proposal mechanism that exploits statistical cues to prioritize promising hypotheses.

Comparison to enumeration and runtime. Alg. 2 explores $\Omega(|\Sigma|^L)$ programs in the worst case, trading exponential *time* for near-optimal sample complexity. By contrast, LLM-ERM replaces exhaustive enumeration with an LLM-guided *propose-verify* loop: the search is effectively restricted to at most k b candidates, each selected using data-informed heuristics (e.g., parity checks, divisibility filters) surfaced by the LLM. While this does not provide worst-case guarantees, the ability of modern "thinking" LLMs to simulate algorithmic strategies, exploit residuals, and adapt proposals yields a practical trade-off: dramatically narrower search, with ERM-style selection preserving the generalization benefits of learning short programs. For runtime, fix k, b, and m, and let $T_{\rm LLM}$ and $T_{\rm ver}$ be the average time for one LLM call and the per-example verification. Each iteration performs one LLM call and verifies up to b candidates on m examples, so the per-iteration cost is $T_{\rm LLM} + b \, m \, T_{\rm ver}$, and the total time is $T_{\rm ime}(k, b, m) = \mathcal{O}\left(k \, T_{\rm LLM} + k \, b \, m \, T_{\rm ver}\right)$. For small m the LLM call dominates; for large m verification dominates. Thus, wall clock time scales linearly in k, b, and m, with constants set by LLM efficiency and verification cost.

Interpretability. LLM-ERM makes both the *learned object* and the *learning process* transparent. Each run returns (i) an *executable program* and (ii) a *reasoning trace* recording candidates, rationales, and residual errors (with train accuracies when the model chose to compute them). Fig. 1 shows a GPT-5-Thinking reasoning trace (taken from the ChatGPT-5 web UI) on IsPrime and Random 10-Parity with 100 samples of 50-digit inputs (see also Fig. 19). The trace ties concrete rules (e.g., parity checks, digit filters, Miller-Rabin) to the errors they address, clarifying *why* a candidate is proposed, *which* mistakes it fixes, and *when* search stops. In particular, failure modes become auditable (e.g., partial solutions on palindromes or Dyck-2), and successes are inspectable, with invariants testable via counterfactual probes. Because the output is symbolic code, we can unit test, stress test out of distribution, or edit and re-run components—turning behavior into an executable, inspectable artifact rather than opaque weights. The trace thus serves as a compact, reproducible *proof of learning*, documenting not only the final program but also the path to it.

4 EXPERIMENTS

We evaluate LLM-ERM's sample efficiency against SGD-trained LLMs on synthetic algorithmic tasks under controlled distributions (e.g., parity, pattern matching, palindromes, Dyck-2, primality, cellular automata; see App. A.1). For each sequence length we use a small-data regime (m=200 labeled examples; 100 train and 100 validation) and test on large held-out sets. LLM-ERM proposes k candidate programs from a pretrained reasoning LLM and selects the one with the lowest validation

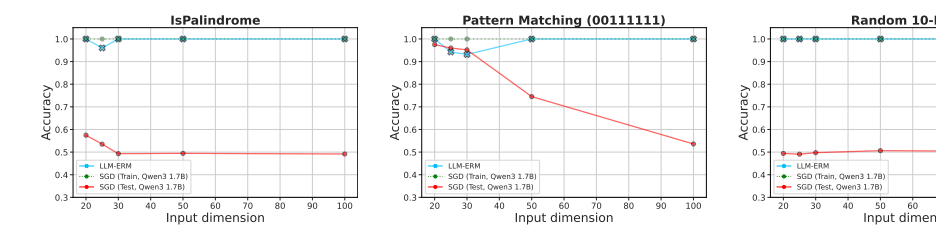


Figure 5: **LLM-ERM generalizes from 200 samples, while an SGD-trained LLM overfits.** With only 200 training examples per task, LLM-ERM typically recovers the target function exactly. For each input length n (x-axis), models are trained and tested independently on sequences of that length. Although training Qwen3-1.7B from scratch with SGD fits the training data at each n, it fails to generalize as n grows. For Random 10-Parity, the 10 indices used for the parity check are fixed by seed 42, while the overall input length n varies. See Fig. 11 in App. A.2 for additional results.

Task	n=20		n	n=25		n=30		n=50		n=100	
	Baseline	LLM-ERM									
Full Parity	50.5%	∞%	50.1%	∞%	50.1%	∞%	50.0%	∞%	49.3%	∞%	
First-Half Parity	51.0%	100%	51.3%	100%	48.9%	100%	50.5%	100%	50.6%	100%	
Random 3-Parity	49.8%	100%	50.5%	100%	50.4%	100%	49.9%	100%	49.7%	100%	
Random 10-Parity	49.4%	100%	49.1%	100%	49.8%	100%	50.6%	100%	50.3%	100%	
Pattern Matching (10101010)	91.4%	∞%	82.8%	98.9%	57.8%	98.5%	58.7%	∞%	51.5%	∞%	
Pattern Matching (00111111)	97.5%	∞ %	96.0%	94.2%	95.2%	93.2%	74.5%	∞ %	53.6%	∞ %	
IsPalindrome	57.5%	100%	53.5%	96.0%	49.3%	100%	49.4%	100%	49.2%	100%	
Dyck-2*	59.8%	77.4%	58.0%	90.5%	53.0%	80.0%	51.1%	90.5%	51.4%	80.1%	
IsPrime	88.5%	∞ %	88.5%	∞ %	87.8%	∞ %	89.9%	∞ %	90.3%	∞ %	
IsPrime (Ends in {1, 3, 7, 9})	59.9%	∞ %	60.2%	∞ %	57.0%	∞ %	57.0%	∞ %	58.8%	∞ %	
Cellular Automata Parity [⋄]	49.4%	100%	50.1%	100%	49.8%	∞ %	50.5%	∞ %	49.4%	∞ %	
SHA-256 Parity	48.3%	50.2%	50.2%	49.9%	50.5%	50.4%	50.3%	50.0%	49.8%	50.1%	

^{*}For Dyck-2, lengths are $n = \{20, 40, 60, 80, 100\}$ respectively.

Table 1: **Test accuracy of SGD-trained LLMs vs. LLM-ERM.** The baseline model attains 100% training accuracy on all tasks but fails to generalize, often collapsing to chance-level performance (\approx 50%). By contrast, LLM-ERM achieves near-perfect generalization by synthesizing functionally correct programs. In some cases, LLM-ERM produces dimension-invariant Python programs; in these cases, test accuracy is denoted as ∞ %.

error, while baselines are transformers trained from scratch with SGD on the same data. Unless noted otherwise, hyperparameters and preprocessing are held fixed across tasks.

LLM training details. We train LLMs from scratch as binary classifiers h for targets $y: \mathcal{X} \to \{0,1\}$. We draw m i.i.d. samples $S = \{(x_i,y(x_i))\}_{i=1}^m$ where $\mathcal{X} = \{0,1\}^n$ or $\mathcal{X} = \{0,\dots,9\}^n$. Each pair $(x_i,y(x_i))$ is represented as a sequence of length n+1: the model reads $x_i = (x_{i,1},\dots,x_{i,n})$ and predicts $y(x_i)$. We optimize binary cross-entropy between the model's logits and the ground-truth labels using the AdamW optimizer (Loshchilov and Hutter, 2019).

In our main training from-scratch experiments, which use Qwen3-1.7B, the models are trained on $m_{\text{train}}=200$ examples for 200 epochs with a batch size of 20 and a cosine annealing learning rate scheduler (Loshchilov and Hutter, 2019) (with $\eta_{\text{max}}=10^{-5}$, $\eta_{\text{min}}=10^{-6}$). The model is tested on sequence lengths $n \in \{20, 25, 30, 50, 100\}$ with a held-out set of $m_{\text{test}}=10,000$ examples. For a separate large-scale data ablation, we trained a custom 75.7M parameter model based on the BLOOM architecture (Scao et al., 2023) (hidden dim 512, 8 heads, 24 layers). This BLOOM-75M model was trained on a much larger dataset of $m_{\text{train}}=100k$ samples for 1000 epochs, using a batch size of 256 and a constant learning rate of $\eta=10^{-5}$. All runs use bfloat16 on a single node with two 94 GB NVIDIA H100 GPUs.

Model architecture. For the baseline, we train a <code>Qwen3-1.7B</code> model (Yang et al., 2025) from scratch, adapted to binary classification: the vocabulary is restricted to three tokens (<code>vocab_size=3</code>) and the language-modeling head is replaced by a single linear layer (hidden_size→1). The network has 28 transformer blocks, 16 attention heads, and hidden size 2048 (about 1.4B parameters). See Fig. 12 (App. A.2.1) for additional experiments with <code>Llama-3.2-lB</code> (Meta AI, 2024; Grattafiori et al., 2024) and <code>DeepSeek-Coder-1.3B</code> (Guo et al., 2024).

For Cellular Automata Parity, length $n=\{100\}$ took k=27 attempts.

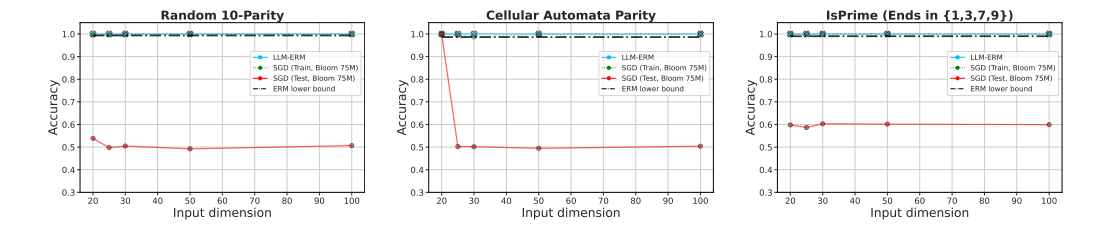


Figure 6: SGD-trained LLMs struggle on algorithmic tasks even with 100k samples. We train BLOOM-75M on Random 10-Parity (left), Cellular Automata Parity (middle), and IsPrime with negatives restricted to $\{1,3,7,9\}$ (right), each with 100k examples. Despite abundant data and perfect fitting, the model still overfits and fails to generalize. The ERM lower bound is computed as $\frac{1}{m}[L\log|\Sigma| + \log(\frac{2L^2}{\delta})]$ with δ =10⁻¹⁰, $|\Sigma|$ =128 (ASCII), and L the length of a short Python program implementing the target.

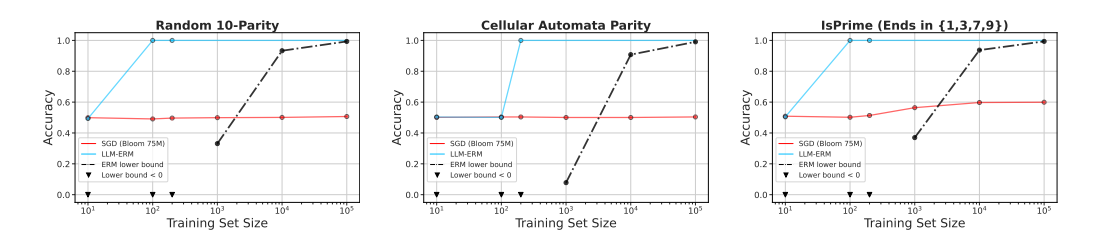


Figure 7: SGD-trained LLMs can fail to learn algorithmic tasks even with 100k examples; LLM-ERM succeeds with 200. We compare the test performance of LLM-ERM and SGD-training of BLOOM-75M on Random 10-Parity (left), Cellular Automata Parity (middle), and IsPrime (Ends in {1,3,7,9}) (right) when varying the training set size. SGD training of BLOOM-75M overfits, with test accuracy near chance across all training sizes. LLM-ERM achieves 100% test accuracy with just 200 examples.

Evaluation tasks. We use several binary algorithmic problems spanning (i) local pattern detection, (ii) global XOR–style dependencies (parity function variants), (iii) symmetry/mirroring (palindrome detection), (iv) context-free parsing (Dyck-2), (v) and number-theoretic predicates (primality). For each sequence length, datasets are class-balanced with equal positives and negatives (see App. A.1 for formal definitions and data-generation procedures). In essence, each task presents a different challenge for learning complex reasoning patterns. We systematically test generalization across tasks and analyze performance over varying input lengths and training durations.

LLM-ERM. Our method (Alg. 1, illustrated in Fig. 3) leverages in-context program synthesis with a pretrained LLM (GPT-5). We split S into equal-sized training $S_{\rm tr}$ and validation sets $S_{\rm val}$ (of size $m_{\rm train}=m_{\rm validation}$). The training split conditions the prompt in Fig. 4, which we submit to the LLM as shown in Fig. 3. The generation process is configured with reasoning_effort = High, text_verbosity=Low, max tokens 20k, and a per call timeout 20 mins. Temperature and top-p are managed by the platform and are not user-configurable. We generate up to k=5 candidate responses with batch sizes b=1 and evaluate each on the validation set. We set $\theta=0$ and stopped once validation error reached zero. If no perfect program appeared, we keep the candidate with the lowest validation error overall.

RESULTS

We observe a sharp performance split between the SGD baseline and LLM-ERM. SGD often reaches perfect training accuracy yet fails to generalize. In contrast, LLM-ERM reliably recovers the underlying rule from only a few examples and generalizes well. We summarize the results in Tab. 1.

SGD fails to generalize. The baseline, a <code>Qwen3-1.7B</code> model trained from scratch, exhibited obvious signs of severe overfitting. Across all tasks and sequence lengths, the model achieved 100% training accuracy, indicating sufficient capacity to memorize the 200 training examples. However, its

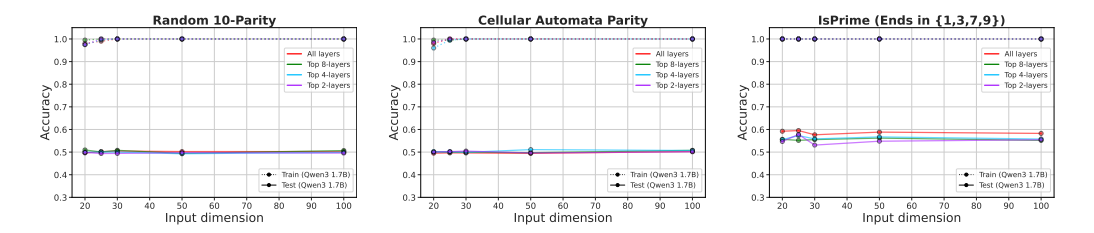


Figure 8: Fine-tuning pre-trained LLMs fails to overcome overfitting on algorithmic tasks. We fine-tuned <code>Qwen3-1.7B</code> on three tasks with 200 samples, training either the full model or only the top 2, 4, or 8 layers. While the models could fit the data, their test accuracy remained near 50%. See Fig. 13 in App. A.2.2 for additional results.

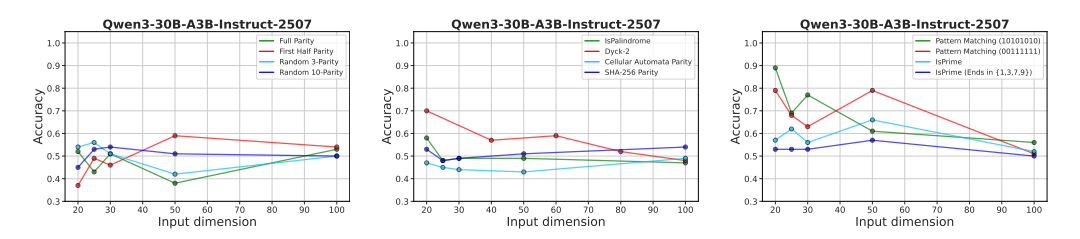


Figure 9: Test accuracy for in-context learning with three large models also fails to generalize. The plots display the performance of <code>Qwen3-30B-A3B-Instruct-2507</code> on all tasks when provided with 200 training examples in-context. Almost all of the observed test accuracy remains near the 50% chance baseline across all tested sequence lengths. See Fig. 14 in App. A.2.3 for additional results.

performance on the held-out test set of 10,000 samples generally shows a near-total failure to learn the underlying algorithmic principles.

Failure on non-local and recursive tasks. For tasks requiring non-local reasoning or recursive structures, the model's performance was statistically indistinguishable from random guessing. On all variants of parity (Full, First-Half, Random 3- and 10-Parity), Palindrome Recognition, and Double Parentheses (Dyck-2 language), the test accuracy hovered around 50% (see Fig. 5 as well as Tab. 1 and Fig. 11 for the complete results). This indicates a catastrophic failure to generalize. The model did not capture the global property of parity, the symmetrical structure of palindromes, or the context-free grammar of the Dyck language, instead relying on memorization of the training data.

SGD has limited success on local/heuristic tasks. The model succeeds mainly when simple local cues suffice. In Pattern Matching, accuracy is high at small n but collapses as n grows: for 001111111, 97.5% at $n{=}20$ vs. 53.6% at $n{=}100$; for 10101010, 91.4% at $n{=}20$ vs. 51.5% at $n{=}100$. This indicates the model likely learned a brittle local detector rather than a robust search procedure. For IsPrime, $\approx 90\%$ test accuracy largely reflects a last-digit heuristic (last digits 0, 2, 4, 5, 6, 8 imply non-prime), which alone yields $\approx 80\%$ on a balanced distribution. When we restrict all negatives to end in $\{1, 3, 7, 9\}$, accuracy drops to $\approx 60\%$ (a pure last-digit rule would be $\approx 50\%$), confirming heavy reliance on the final digit.

Scaling to 100k samples does not fix overfitting. With sufficient training data, SGD is expected to generalize well, assuming it can fit the training set. While LLM-ERM learns these tasks (except SHA-256 Parity) from 200 samples, we test whether SGD can match this with $500 \times$ more data. Fig. 6 and Tab. 5 in App. A.2.5 show that an SGD-trained BLOOM-75M still overfits: Random 10-Parity and Cellular Automata Parity remain near chance, and IsPrime stays weak when negative samples are constrained to end in a digit from $\{1,3,7,9\}$. Thus, even with 100k samples, SGD fails to generalize. The ERM lower bound, based on Prop. 1, is computed as $1 - \frac{1}{m} [L \log |\Sigma| + \log(\frac{2L^2}{\delta})]$ with m=100k, $\delta=10^{-10}$, $|\Sigma|=128$ (ASCII), and L the length of a short Python program for the target function. This bound guarantees that Alg. 2 performs near 100% at test time when m=100k. However, SGD does not generalize, whereas LLM-ERM learns these tasks perfectly with only 200 samples.

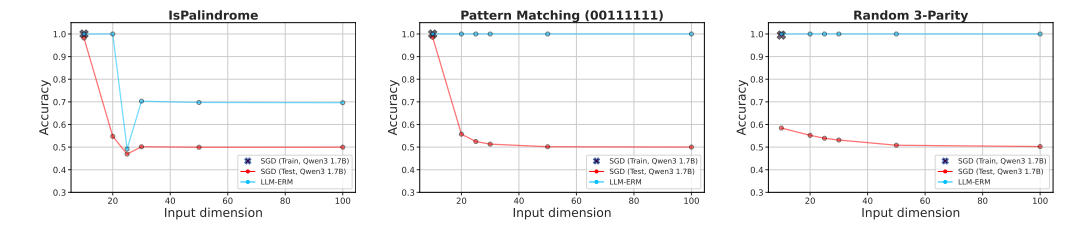


Figure 10: **LLM-ERM exhibits remarkable degrees of length generalization.** We evaluate performance on IsPalindrome (left), Pattern Matching (middle), and Random 3-Parity (right). Both models are trained on a dataset of 200 samples with fixed input dimension (d=10) and evaluated on inputs with dimensions up to 100. The baseline fits the training distribution but collapses to $\approx 50\%$ accuracy at larger dimensions. In contrast, LLM-ERM synthesizes dimension-invariant programs for Pattern Matching and Random 3-Parity.

In addition to the plots above, we conducted an experiment varying the training set size from 10 to 100k examples. As shown in Fig. 7 (see also Tab. 6), training from scratch struggles to learn even with 100k examples, whereas LLM-ERM achieves perfect generalization with as few as 200 samples.

Fine-tuning and in-context learning are insufficient for program learning. A natural follow-up question to the results in Fig. 5 is whether the same behavior holds for pre-trained LLMs. To examine this, we conducted similar experiments involving fine-tuning (Fig. 8) and in-context learning (Fig. 9).

For fine-tuning, we used $\approx 1B$ -parameter pretrained LLMs, trained on 200 samples for 1,000 epochs with AdamW (Loshchilov and Hutter, 2019) and a cosine-annealing LR scheduler (Loshchilov and Hutter, 2019). Learning rate and batch size were selected by grid search. We evaluated four settings: full fine-tuning and partial fine-tuning of the top 2, 4, or 8 Transformer blocks. For in-context learning, we used $\approx 30B$ -parameter pretrained LLMs. The models were prompted with the problem statement (see Fig. 15 in App. A.2.3) together with all 200 training examples, and tasked with predicting the label of a single test input.

Both approaches failed to generalize. Although fine-tuning achieved high training accuracy, test performance on non-local tasks remained near chance ($\approx 50\%$), a result mirrored in the in-context learning experiments. Partial success was observed in both settings on certain tasks, such as Pattern Matching and Dyck-2. Full experimental details and results are provided in App. A.2.2 and A.2.3.

Achieving perfect algorithmic discovery via LLM-ERM. For the most complex tasks, LLM-ERM succeeded where SGD failed completely. On all Parity variants, Palindrome Recognition, and Primality, the method consistently generated a functionally correct Python program, achieving 100% test accuracy across all sequence lengths. These results demonstrate the ability of LLM-guided synthesis to move beyond statistical correlation and perform genuine algorithmic induction. In Tab. 1 we numerically compare the two methods, where our method achieves perfect algorithmic discovery on several tasks, including parity variants and primality testing (we denote that by $\infty\%$).

LLM-ERM exhibits remarkable degrees of length generalization. To further understand the performance gap between SGD and LLM-ERM, we conducted several experiments on the two algorithms' out-of-distribution generalization. Specifically, we investigated whether the algorithms exhibit some degree of length generalization. To test length generalization, we trained models exclusively on a fixed input length (n=10) and evaluated them on longer, unseen sequences. As shown in Fig. 10 (and Tab. 4 in App. A.2.4), the SGD baseline overfits severely to the training length, with its accuracy collapsing to chance on longer inputs. In contrast, LLM-ERM identifies dimension-invariant solutions that generalize robustly.

Additional experiments. We performed additional experiments and ablations with training various architectures from scratch (App. A.2.1), fine-tuning (App. A.2.2), in-context learning (A.2.3), length generalization (App. A.2.4), data scaling (App. A.2.5), as well as varying batch sizes (App. A.2.6) and learning rates (App. A.2.7). Across the different settings, results are consistent: standard approaches (SGD, fine-tuning, in-context learning) fail to generalize on sparse, non-local tasks and learn only length-dependent heuristics on Pattern Matching and IsPalindrome (App. A.2).

REFERENCES

- E. Abbe, P. Kamath, E. Malach, C. Sandon, and N. Srebro. On the power of differentiable learning versus pac and sq learning. In M. Ranzato, A. Beygelzimer, Y. Dauphin, P. Liang, and J. W. Vaughan, editors, *Advances in Neural Information Processing Systems*, volume 34, pages 24340–24351. Curran Associates, Inc., 2021. URL https://proceedings.neurips.cc/paper_files/paper/2021/file/cc225865b743ecc91c4743259813f604-Paper.pdf.
- E. Akyürek, D. Schuurmans, J. Andreas, T. Ma, and D. Zhou. What learning algorithm is in-context learning? investigations with linear models. In *The Eleventh International Conference on Learning Representations*, 2023. URL https://openreview.net/forum?id=0g0X4H8yN4I.
- B. Barak, B. L. Edelman, S. Goel, S. M. Kakade, eran malach, and C. Zhang. Hidden progress in deep learning: SGD learns parities near the computational limit. In A. H. Oh, A. Agarwal, D. Belgrave, and K. Cho, editors, *Advances in Neural Information Processing Systems*, 2022. URL https://openreview.net/forum?id=8XWP2ewX-im.
- A. Barron and T. Cover. Minimum complexity density estimation. *IEEE Transactions on Information Theory*, 37(4):1034–1054, 1991. doi: 10.1109/18.86996.
- A. Barron, J. Rissanen, and B. Yu. The minimum description length principle in coding and modeling. *IEEE Transactions on Information Theory*, 44(6):2743–2760, 1998. doi: 10.1109/18.720554.
- S. Bhansali, A. Jin, T. Lizzo, and L. Heck. Lego: Language model building blocks, 2024. URL https://arxiv.org/abs/2410.18287.
- A. Blum, M. Furst, J. Jackson, M. Kearns, Y. Mansour, and S. Rudich. Weakly learning dnf and characterizing statistical query learning using fourier analysis. In *Proceedings of the Twenty-Sixth Annual ACM Symposium on Theory of Computing*, STOC '94, page 253–262, New York, NY, USA, 1994. Association for Computing Machinery. ISBN 0897916638. doi: 10.1145/195058.195147. URL https://doi.org/10.1145/195058.195147.
- A. Blum, A. Kalai, and H. Wasserman. Noise-tolerant learning, the parity problem, and the statistical query model. *J. ACM*, 50(4):506–519, July 2003. ISSN 0004-5411. doi: 10.1145/792538.792543. URL https://doi.org/10.1145/792538.792543.
- A. Blumer, A. Ehrenfeucht, D. Haussler, and M. K. Warmuth. Occam's razor. *Information Processing Letters*, 24(6):377–380, 1987. ISSN 0020-0190. doi: https://doi.org/10.1016/0020-0190(87)90114-1. URL https://www.sciencedirect.com/science/article/pii/0020019087901141.
- L. Bottou. Large-scale machine learning with stochastic gradient descent. In *Proceedings of COMPSTAT'2010*, pages 177–186. Physica Verlag, 2010.
- T. Brown, B. Mann, N. Ryder, M. Subbiah, J. D. Kaplan, P. Dhariwal, A. Neelakantan, P. Shyam, G. Sastry, A. Askell, S. Agarwal, A. Herbert-Voss, G. Krueger, T. Henighan, R. Child, A. Ramesh, D. Ziegler, J. Wu, C. Winter, C. Hesse, M. Chen, E. Sigler, M. Litwin, S. Gray, B. Chess, J. Clark, C. Berner, S. McCandlish, A. Radford, I. Sutskever, and D. Amodei. Language models are few-shot learners. In H. Larochelle, M. Ranzato, R. Hadsell, M. Balcan, and H. Lin, editors, Advances in Neural Information Processing Systems, volume 33, pages 1877–1901. Curran Associates, Inc., 2020. URL https://proceedings.neurips.cc/paper_files/paper/2020/file/1457c0d6bfcb4967418bfb8ac142f64a-Paper.pdf.
- X. Chen, M. Lin, N. Schärli, and D. Zhou. Teaching large language models to self-debug. In The Twelfth International Conference on Learning Representations, 2024. URL https://openreview.net/forum?id=KuPixIqPiq.
- A. Daniely. Sgd learns the conjugate kernel class of the network. In *Proceedings of the 31st International Conference on Neural Information Processing Systems*, NIPS'17, page 2419–2427, Red Hook, NY, USA, 2017. Curran Associates Inc. ISBN 9781510860964.
- A. Daniely and E. Malach. Learning parities with neural networks. In *Proceedings of the 34th International Conference on Neural Information Processing Systems*, NIPS '20, Red Hook, NY, USA, 2020. Curran Associates Inc. ISBN 9781713829546.

- A. de Wynter. Is in-context learning learning?, 2025. URL https://arxiv.org/abs/2509. 10414.
- DeepMind. Alphaevolve: A gemini-powered coding agent for designing advanced algorithms, 2025. URL https://deepmind.google/discover/blog/alphaevolve-a-gemini-powered-coding-agent-for-designing-advanced-algorithms.
- V. Feldman. A general characterization of the statistical query complexity. In S. Kale and O. Shamir, editors, *Proceedings of the 2017 Conference on Learning Theory*, volume 65 of *Proceedings of Machine Learning Research*, pages 785–830. PMLR, 07–10 Jul 2017. URL https://proceedings.mlr.press/v65/feldman17c.html.
- V. Feldman, E. Grigorescu, L. Reyzin, S. S. Vempala, and Y. Xiao. Statistical algorithms and a lower bound for detecting planted cliques. *J. ACM*, 64(2), Apr. 2017. ISSN 0004-5411. doi: 10.1145/3046674. URL https://doi.org/10.1145/3046674.
- V. Feldman, W. Perkins, and S. Vempala. On the complexity of random satisfiability problems with planted solutions. *SIAM Journal on Computing*, 47(4):1294–1338, 2018. doi: 10.1137/16M1078471. URL https://doi.org/10.1137/16M1078471.
- G. Giapitzakis, K. Fountoulakis, E. Nichani, and J. D. Lee. On the statistical query complexity of learning semiautomata: a random walk approach, 2025. URL https://arxiv.org/abs/2510.04115.
- A. Grattafiori, A. Dubey, A. Jauhri, A. Pandey, A. Kadian, A. Al-Dahle, A. Letman, A. Mathur, A. Schelten, A. Vaughan, A. Yang, A. Fan, A. Goyal, A. Hartshorn, A. Yang, A. Mitra, A. Sravankumar, A. Korenev, A. Hinsvark, A. Rao, A. Zhang, A. Rodriguez, A. Gregerson, A. Spataru, B. Roziere, B. Biron, B. Tang, B. Chern, C. Caucheteux, C. Nayak, C. Bi, C. Marra, C. McConnell, C. Keller, C. Touret, C. Wu, C. Wong, C. C. Ferrer, C. Nikolaidis, D. Allonsius, D. Song, D. Pintz, D. Livshits, D. Wyatt, D. Esiobu, D. Choudhary, D. Mahajan, D. Garcia-Olano, D. Perino, D. Hupkes, E. Lakomkin, E. AlBadawy, E. Lobanova, E. Dinan, E. M. Smith, F. Radenovic, F. Guzmán, F. Zhang, G. Synnaeve, G. Lee, G. L. Anderson, G. Thattai, G. Nail, G. Mialon, G. Pang, G. Cucurell, H. Nguyen, H. Korevaar, H. Xu, H. Touvron, I. Zarov, I. A. Ibarra, I. Kloumann, I. Misra, I. Evtimov, J. Zhang, J. Copet, J. Lee, J. Geffert, J. Vranes, J. Park, J. Mahadeokar, J. Shah, J. van der Linde, J. Billock, J. Hong, J. Lee, J. Fu, J. Chi, J. Huang, J. Liu, J. Wang, J. Yu, J. Bitton, J. Spisak, J. Park, J. Rocca, J. Johnstun, J. Saxe, J. Jia, K. V. Alwala, K. Prasad, K. Upasani, K. Plawiak, K. Li, K. Heafield, K. Stone, K. El-Arini, K. Iyer, K. Malik, K. Chiu, K. Bhalla, K. Lakhotia, L. Rantala-Yeary, L. van der Maaten, L. Chen, L. Tan, L. Jenkins, L. Martin, L. Madaan, L. Malo, L. Blecher, L. Landzaat, L. de Oliveira, M. Muzzi, M. Pasupuleti, M. Singh, M. Paluri, M. Kardas, M. Tsimpoukelli, M. Oldham, M. Rita, M. Pavlova, M. Kambadur, M. Lewis, M. Si, M. K. Singh, M. Hassan, N. Goyal, N. Torabi, N. Bashlykov, N. Bogoychev, N. Chatterji, N. Zhang, O. Duchenne, O. Çelebi, P. Alrassy, P. Zhang, P. Li, P. Vasic, P. Weng, P. Bhargava, P. Dubal, P. Krishnan, P. S. Koura, P. Xu, Q. He, Q. Dong, R. Srinivasan, R. Ganapathy, R. Calderer, R. S. Cabral, R. Stojnic, R. Raileanu, R. Maheswari, R. Girdhar, R. Patel, R. Sauvestre, R. Polidoro, R. Sumbaly, R. Taylor, R. Silva, R. Hou, R. Wang, S. Hosseini, S. Chennabasappa, S. Singh, S. Bell, S. S. Kim, S. Edunov, S. Nie, S. Narang, S. Raparthy, S. Shen, S. Wan, S. Bhosale, S. Zhang, S. Vandenhende, S. Batra, S. Whitman, S. Sootla, S. Collot, S. Gururangan, S. Borodinsky, T. Herman, T. Fowler, T. Sheasha, T. Georgiou, T. Scialom, T. Speckbacher, T. Mihaylov, T. Xiao, U. Karn, V. Goswami, V. Gupta, V. Ramanathan, V. Kerkez, V. Gonguet, V. Do, V. Vogeti, V. Albiero, V. Petrovic, W. Chu, W. Xiong, W. Fu, W. Meers, X. Martinet, X. Wang, X. Wang, X. E. Tan, X. Xia, X. Xie, X. Jia, X. Wang, Y. Goldschlag, Y. Gaur, Y. Babaei, Y. Wen, Y. Song, Y. Zhang, Y. Li, Y. Mao, Z. D. Coudert, Z. Yan, Z. Chen, Z. Papakipos, A. Singh, A. Srivastava, A. Jain, A. Kelsey, A. Shajnfeld, A. Gangidi, A. Victoria, A. Goldstand, A. Menon, A. Sharma, A. Boesenberg, A. Baevski, A. Feinstein, A. Kallet, A. Sangani, A. Teo, A. Yunus, A. Lupu, A. Alvarado, A. Caples, A. Gu, A. Ho, A. Poulton, A. Ryan, A. Ramchandani, A. Dong, A. Franco, A. Goyal, A. Saraf, A. Chowdhury, A. Gabriel, A. Bharambe, A. Eisenman, A. Yazdan, B. James, B. Maurer, B. Leonhardi, B. Huang, B. Loyd, B. D. Paola, B. Paranjape, B. Liu, B. Wu, B. Ni, B. Hancock, B. Wasti, B. Spence, B. Stojkovic, B. Gamido, B. Montalvo, C. Parker, C. Burton, C. Mejia, C. Liu, C. Wang, C. Kim, C. Zhou, C. Hu, C.-H. Chu, C. Cai, C. Tindal, C. Feichtenhofer, C. Gao, D. Civin, D. Beaty, D. Kreymer, D. Li, D. Adkins, D. Xu, D. Testuggine, D. David, D. Parikh, D. Liskovich, D. Foss, D. Wang, D. Le, D. Holland, E. Dowling, E. Jamil, E. Montgomery, E. Presani, E. Hahn, E. Wood,

- E.-T. Le, E. Brinkman, E. Arcaute, E. Dunbar, E. Smothers, F. Sun, F. Kreuk, F. Tian, F. Kokkinos, F. Ozgenel, F. Caggioni, F. Kanayet, F. Seide, G. M. Florez, G. Schwarz, G. Badeer, G. Swee, G. Halpern, G. Herman, G. Sizov, Guangyi, Zhang, G. Lakshminarayanan, H. Inan, H. Shojanazeri, H. Zou, H. Wang, H. Zha, H. Habeeb, H. Rudolph, H. Suk, H. Aspegren, H. Goldman, H. Zhan, I. Damlaj, I. Molybog, I. Tufanov, I. Leontiadis, I.-E. Veliche, I. Gat, J. Weissman, J. Geboski, J. Kohli, J. Lam, J. Asher, J.-B. Gaya, J. Marcus, J. Tang, J. Chan, J. Zhen, J. Reizenstein, J. Teboul, J. Zhong, J. Jin, J. Yang, J. Cummings, J. Carvill, J. Shepard, J. McPhie, J. Torres, J. Ginsburg, J. Wang, K. Wu, K. H. U, K. Saxena, K. Khandelwal, K. Zand, K. Matosich, K. Veeraraghavan, K. Michelena, K. Li, K. Jagadeesh, K. Huang, K. Chawla, K. Huang, L. Chen, L. Garg, L. A, L. Silva, L. Bell, L. Zhang, L. Guo, L. Yu, L. Moshkovich, L. Wehrstedt, M. Khabsa, M. Avalani, M. Bhatt, M. Mankus, M. Hasson, M. Lennie, M. Reso, M. Groshev, M. Naumov, M. Lathi, M. Keneally, M. Liu, M. L. Seltzer, M. Valko, M. Restrepo, M. Patel, M. Vyatskov, M. Samvelyan, M. Clark, M. Macey, M. Wang, M. J. Hermoso, M. Metanat, M. Rastegari, M. Bansal, N. Santhanam, N. Parks, N. White, N. Bawa, N. Singhal, N. Egebo, N. Usunier, N. Mehta, N. P. Laptev, N. Dong, N. Cheng, O. Chernoguz, O. Hart, O. Salpekar, O. Kalinli, P. Kent, P. Parekh, P. Saab, P. Balaji, P. Rittner, P. Bontrager, P. Roux, P. Dollar, P. Zvyagina, P. Ratanchandani, P. Yuvraj, Q. Liang, R. Alao, R. Rodriguez, R. Ayub, R. Murthy, R. Nayani, R. Mitra, R. Parthasarathy, R. Li, R. Hogan, R. Battey, R. Wang, R. Howes, R. Rinott, S. Mehta, S. Siby, S. J. Bondu, S. Datta, S. Chugh, S. Hunt, S. Dhillon, S. Sidorov, S. Pan, S. Mahajan, S. Verma, S. Yamamoto, S. Ramaswamy, S. Lindsay, S. Lindsay, S. Feng, S. Lin, S. C. Zha, S. Patil, S. Shankar, S. Zhang, S. Zhang, S. Wang, S. Agarwal, S. Sajuyigbe, S. Chintala, S. Max, S. Chen, S. Kehoe, S. Satterfield, S. Govindaprasad, S. Gupta, S. Deng, S. Cho, S. Virk, S. Subramanian, S. Choudhury, S. Goldman, T. Remez, T. Glaser, T. Best, T. Koehler, T. Robinson, T. Li, T. Zhang, T. Matthews, T. Chou, T. Shaked, V. Vontimitta, V. Ajayi, V. Montanez, V. Mohan, V. S. Kumar, V. Mangla, V. Ionescu, V. Poenaru, V. T. Mihailescu, V. Ivanov, W. Li, W. Wang, W. Jiang, W. Bouaziz, W. Constable, X. Tang, X. Wu, X. Wang, X. Wu, X. Gao, Y. Kleinman, Y. Chen, Y. Hu, Y. Jia, Y. Qi, Y. Li, Y. Zhang, Y. Zhang, Y. Adi, Y. Nam, Yu, Wang, Y. Zhao, Y. Hao, Y. Qian, Y. Li, Y. He, Z. Rait, Z. DeVito, Z. Rosnbrick, Z. Wen, Z. Yang, Z. Zhao, and Z. Ma. The llama 3 herd of models, 2024. URL https://arxiv.org/abs/2407.21783.
- D. Guo, Q. Zhu, D. Yang, Z. Xie, K. Dong, W. Zhang, G. Chen, X. Bi, Y. Wu, Y. K. Li, F. Luo, Y. Xiong, and W. Liang. Deepseek-coder: When the large language model meets programming the rise of code intelligence. *CoRR*, abs/2401.14196, 2024. URL http://dblp.uni-trier.de/db/journals/corr/corr2401.html#abs-2401-14196.
- H. Hu, C. He, H. Zhang, X. Xie, and Q. Zhang. Aprmcts: Improving llm-based automated program repair with iterative tree search, 2025. URL https://arxiv.org/abs/2507.01827.
- M. Kearns. Efficient noise-tolerant learning from statistical queries. J. ACM, 45(6):983–1006, Nov. 1998. ISSN 0004-5411. doi: 10.1145/293347.293351. URL https://doi.org/10.1145/293347.293351.
- A. Klivans and P. Kothari. Embedding Hard Learning Problems Into Gaussian Space. In K. Jansen, J. Rolim, N. R. Devanur, and C. Moore, editors, *Approximation, Randomization, and Combinatorial Optimization. Algorithms and Techniques (APPROX/RANDOM 2014)*, volume 28 of *Leibniz International Proceedings in Informatics (LIPIcs)*, pages 793–809, Dagstuhl, Germany, 2014. Schloss Dagstuhl Leibniz-Zentrum für Informatik. ISBN 978-3-939897-74-3. doi: 10.4230/LIPIcs.APPROX-RANDOM.2014.793. URL https://drops.dagstuhl.de/entities/document/10.4230/LIPIcs.APPROX-RANDOM.2014.793.
- A. R. Klivans and A. A. Sherstov. Unconditional lower bounds for learning intersections of halfspaces. *Machine Learning*, 69(2-3):97–114, 2007. doi: 10.1007/s10994-007-5010-1.
- L. A. Levin. Universal sequential search problems. *Problems of Information Transmission (Problemy Peredachi Informatsii)*, 9(3):115–116 (Russian original) / 265–266 (English translation), 1973. URL https://www.mathnet.ru/eng/ppi914.
- I. Loshchilov and F. Hutter. Decoupled weight decay regularization. In *International Conference on Learning Representations*, 2019. URL https://openreview.net/forum?id=Bkg6RiCqY7.

- A. Madaan, N. Tandon, P. Gupta, S. Hallinan, L. Gao, S. Wiegreffe, U. Alon, N. Dziri, S. Prabhumoye, Y. Yang, S. Gupta, B. P. Majumder, K. Hermann, S. Welleck, A. Yazdanbakhsh, and P. Clark. Self-refine: iterative refinement with self-feedback. In *Proceedings of the 37th International Conference on Neural Information Processing Systems*, NIPS '23, Red Hook, NY, USA, 2023. Curran Associates Inc.
- D. A. McAllester. Some pac-bayesian theorems. In *Proceedings of the Eleventh Annual Conference on Computational Learning Theory*, COLT' 98, page 230–234, New York, NY, USA, 1998. Association for Computing Machinery. ISBN 1581130570. doi: 10.1145/279943.279989. URL https://doi.org/10.1145/279943.279989.
- Meta AI. Llama 3.2: Revolutionizing edge ai and vision with open, multimodal models. Meta AI Blog, Sept. 2024. URL https://ai.meta.com/blog/llama-3-2-connect-2024-vision-edge-mobile-devices/.
- S. Min, X. Lyu, A. Holtzman, M. Artetxe, M. Lewis, H. Hajishirzi, and L. Zettlemoyer. Rethinking the role of demonstrations: What makes in-context learning work? In Y. Goldberg, Z. Kozareva, and Y. Zhang, editors, *Proceedings of the 2022 Conference on Empirical Methods in Natural Language Processing*, pages 11048–11064, Abu Dhabi, United Arab Emirates, Dec. 2022. Association for Computational Linguistics. doi: 10.18653/v1/2022.emnlp-main.759. URL https://aclanthology.org/2022.emnlp-main.759/.
- A. Novikov, N. Vũ, M. Eisenberger, E. Dupont, P.-S. Huang, A. Z. Wagner, S. Shirobokov, B. Kozlovskii, F. J. R. Ruiz, A. Mehrabian, M. P. Kumar, A. See, S. Chaudhuri, G. Holland, A. Davies, S. Nowozin, P. Kohli, and M. Balog. Alphaevolve: A coding agent for scientific and algorithmic discovery, 2025. URL https://arxiv.org/abs/2506.13131.
- J. Pourcel, C. Colas, and P.-Y. Oudeyer. Self-improving language models for evolutionary program synthesis: A case study on ARC-AGI. In *Forty-second International Conference on Machine Learning*, 2025. URL https://openreview.net/forum?id=z4IG090qt2.
- A. Power, Y. Burda, H. Edwards, I. Babuschkin, and V. Misra. Grokking: Generalization beyond overfitting on small algorithmic datasets. *arXiv preprint arXiv:2201.02177*, 2022. URL https://arxiv.org/abs/2201.02177.
- L. Reyzin. Statistical queries and statistical algorithms: Foundations and applications, 2020. URL https://arxiv.org/abs/2004.00557.
- J. Rissanen. Stochastic Complexity in Statistical Inquiry Theory. World Scientific Publishing Co., Inc., USA, 1989. ISBN 981020311X.
- H. Robbins and S. Monro. A stochastic approximation method. *Annals of Mathematical Statistics*, 22(3):400–407, 1951. doi: 10.1214/aoms/1177729586.
- I. Safran and O. Shamir. Spurious local minima are common in two-layer ReLU neural networks. In J. Dy and A. Krause, editors, *Proceedings of the 35th International Conference on Machine Learning*, volume 80 of *Proceedings of Machine Learning Research*, pages 4433–4441. PMLR, 10–15 Jul 2018. URL https://proceedings.mlr.press/v80/safran18a.html.
- T. L. Scao, A. Fan, C. Akiki, E. Pavlick, S. Ilić, D. Hesslow, R. Castagné, A. S. Luccioni, F. Yvon, M. Gallé, J. Tow, A. M. Rush, S. Biderman, A. Webson, P. S. Ammanamanchi, T. Wang, B. Sagot, N. Muennighoff, A. V. del Moral, O. Ruwase, R. Bawden, S. Bekman, A. McMillan-Major, I. Beltagy, H. Nguyen, L. Saulnier, S. Tan, P. O. Suarez, V. Sanh, H. Laurençon, Y. Jernite, J. Launay, M. Mitchell, C. Raffel, A. Gokaslan, A. Simhi, A. Soroa, A. F. Aji, A. Alfassy, A. Rogers, A. K. Nitzav, C. Xu, C. Mou, C. Emezue, C. Klamm, C. Leong, D. van Strien, D. I. Adelani, D. Radev, E. G. Ponferrada, E. Levkovizh, E. Kim, E. B. Natan, F. D. Toni, G. Dupont, G. Kruszewski, G. Pistilli, H. Elsahar, H. Benyamina, H. Tran, I. Yu, I. Abdulmumin, I. Johnson, I. Gonzalez-Dios, J. de la Rosa, J. Chim, J. Dodge, J. Zhu, J. Chang, J. Frohberg, J. Tobing, J. Bhattacharjee, K. Almubarak, K. Chen, K. Lo, L. V. Werra, L. Weber, L. Phan, L. B. allal, L. Tanguy, M. Dey, M. R. Muñoz, M. Masoud, M. Grandury, M. Šaško, M. Huang, M. Coavoux, M. Singh, M. T.-J. Jiang, M. C. Vu, M. A. Jauhar, M. Ghaleb, N. Subramani, N. Kassner, N. Khamis, O. Nguyen, O. Espejel, O. de Gibert, P. Villegas, P. Henderson, P. Colombo,

P. Amuok, Q. Lhoest, R. Harliman, R. Bommasani, R. L. López, R. Ribeiro, S. Osei, S. Pyysalo, S. Nagel, S. Bose, S. H. Muhammad, S. Sharma, S. Longpre, S. Nikpoor, S. Silberberg, S. Pai, S. Zink, T. T. Torrent, T. Schick, T. Thrush, V. Danchev, V. Nikoulina, V. Laippala, V. Lepercq, V. Prabhu, Z. Alyafeai, Z. Talat, A. Raja, B. Heinzerling, C. Si, D. E. Taşar, E. Salesky, S. J. Mielke, W. Y. Lee, A. Sharma, A. Santilli, A. Chaffin, A. Stiegler, D. Datta, E. Szczechla, G. Chhablani, H. Wang, H. Pandey, H. Strobelt, J. A. Fries, J. Rozen, L. Gao, L. Sutawika, M. S. Bari, M. S. Al-shaibani, M. Manica, N. Nayak, R. Teehan, S. Albanie, S. Shen, S. Ben-David, S. H. Bach, T. Kim, T. Bers, T. Fevry, T. Neeraj, U. Thakker, V. Raunak, X. Tang, Z.-X. Yong, Z. Sun, S. Brody, Y. Uri, H. Tojarieh, A. Roberts, H. W. Chung, J. Tae, J. Phang, O. Press, C. Li, D. Narayanan, H. Bourfoune, J. Casper, J. Rasley, M. Ryabinin, M. Mishra, M. Zhang, M. Shoeybi, M. Peyrounette, N. Patry, N. Tazi, O. Sanseviero, P. von Platen, P. Cornette, P. F. Lavallée, R. Lacroix, S. Rajbhandari, S. Gandhi, S. Smith, S. Requena, S. Patil, T. Dettmers, A. Baruwa, A. Singh, A. Cheveleva, A.-L. Ligozat, A. Subramonian, A. Névéol, C. Lovering, D. Garrette, D. Tunuguntla, E. Reiter, E. Taktasheva, E. Voloshina, E. Bogdanov, G. I. Winata, H. Schoelkopf, J.-C. Kalo, J. Novikova, J. Z. Forde, J. Clive, J. Kasai, K. Kawamura, L. Hazan, M. Carpuat, M. Clinciu, N. Kim, N. Cheng, O. Serikov, O. Antverg, O. van der Wal, R. Zhang, R. Zhang, S. Gehrmann, S. Mirkin, S. Pais, T. Shavrina, T. Scialom, T. Yun, T. Limisiewicz, V. Rieser, V. Protasov, V. Mikhailov, Y. Pruksachatkun, Y. Belinkov, Z. Bamberger, Z. Kasner, A. Rueda, A. Pestana, A. Feizpour, A. Khan, A. Faranak, A. Santos, A. Hevia, A. Unldreaj, A. Aghagol, A. Abdollahi, A. Tammour, A. HajiHosseini, B. Behroozi, B. Ajibade, B. Saxena, C. M. Ferrandis, D. McDuff, D. Contractor, D. Lansky, D. David, D. Kiela, D. A. Nguyen, E. Tan, E. Baylor, E. Ozoani, F. Mirza, F. Ononiwu, H. Rezanejad, H. Jones, I. Bhattacharya, I. Solaiman, I. Sedenko, I. Nejadgholi, J. Passmore, J. Seltzer, J. B. Sanz, L. Dutra, M. Samagaio, M. Elbadri, M. Mieskes, M. Gerchick, M. Akinlolu, M. McKenna, M. Qiu, M. Ghauri, M. Burynok, N. Abrar, N. Rajani, N. Elkott, N. Fahmy, O. Samuel, R. An, R. Kromann, R. Hao, S. Alizadeh, S. Shubber, S. Wang, S. Roy, S. Viguier, T. Le, T. Oyebade, T. Le, Y. Yang, Z. Nguyen, A. R. Kashyap, A. Palasciano, A. Callahan, A. Shukla, A. Miranda-Escalada, A. Singh, B. Beilharz, B. Wang, C. Brito, C. Zhou, C. Jain, C. Xu, C. Fourrier, D. L. Periñán, D. Molano, D. Yu, E. Manjavacas, F. Barth, F. Fuhrimann, G. Altay, G. Bayrak, G. Burns, H. U. Vrabec, I. Bello, I. Dash, J. Kang, J. Giorgi, J. Golde, J. D. Posada, K. R. Sivaraman, L. Bulchandani, L. Liu, L. Shinzato, M. H. de Bykhovetz, M. Takeuchi, M. Pàmies, M. A. Castillo, M. Nezhurina, M. Sänger, M. Samwald, M. Cullan, M. Weinberg, M. D. Wolf, M. Mihaljcic, M. Liu, M. Freidank, M. Kang, N. Seelam, N. Dahlberg, N. M. Broad, N. Muellner, P. Fung, P. Haller, R. Chandrasekhar, R. Eisenberg, R. Martin, R. Canalli, R. Su, R. Su, S. Cahyawijaya, S. Garda, S. S. Deshmukh, S. Mishra, S. Kiblawi, S. Ott, S. Sang-aroonsiri, S. Kumar, S. Schweter, S. Bharati, T. Laud, T. Gigant, T. Kainuma, W. Kusa, Y. Labrak, Y. S. Bajaj, Y. Venkatraman, Y. Xu, Y. Xu, Y. Xu, Z. Tan, Z. Xie, Z. Ye, M. Bras, Y. Belkada, and T. Wolf. Bloom: A 176b-parameter open-access multilingual language model, 2023. URL https://arxiv.org/abs/2211.05100.

- S. Shalev-Shwartz and S. Ben-David. *Understanding Machine Learning: From Theory to Algorithms*. Cambridge University Press, USA, 2014. ISBN 1107057132.
- S. Shalev-Shwartz, O. Shamir, and S. Shammah. Failures of gradient-based deep learning. In *Proceedings of the 34th International Conference on Machine Learning Volume 70*, ICML'17, page 3067–3075. JMLR.org, 2017.
- L. Shen, A. Mishra, and D. Khashabi. Do pre-trained transformers really learn in-context by gradient descent?, 2024. URL https://openreview.net/forum?id=992eLydH8G.
- N. Shinn, F. Cassano, A. Gopinath, K. R. Narasimhan, and S. Yao. Reflexion: language agents with verbal reinforcement learning. In *Thirty-seventh Conference on Neural Information Processing Systems*, 2023. URL https://openreview.net/forum?id=vAElhFcKW6.
- R. J. Solomonoff. A formal theory of inductive inference, part i and ii. *Information and Control*, 7(1-2):1-22, 224-254, 1964. URL https://www.sciencedirect.com/science/article/pii/S0019995864902232. Parts I and II.
- L. G. Valiant. A theory of the learnable. *Commun. ACM*, 27(11):1134–1142, Nov. 1984. ISSN 0001-0782. doi: 10.1145/1968.1972. URL https://doi.org/10.1145/1968.1972.
- V. N. Vapnik. Statistical Learning Theory. Wiley-Interscience, 1998.

- V. N. Vapnik and A. Y. Chervonenkis. On the uniform convergence of relative frequencies of events to their probabilities. *Theory of Probability & Its Applications*, 16(2):264–280, 1971. doi: 10.1137/1116025.
- J. Von Oswald, E. Niklasson, E. Randazzo, J. Sacramento, A. Mordvintsev, A. Zhmoginov, and M. Vladymyrov. Transformers learn in-context by gradient descent. In A. Krause, E. Brunskill, K. Cho, B. Engelhardt, S. Sabato, and J. Scarlett, editors, *Proceedings of the 40th International Conference on Machine Learning*, volume 202 of *Proceedings of Machine Learning Research*, pages 35151–35174. PMLR, 23–29 Jul 2023. URL https://proceedings.mlr.press/v202/von-oswald23a.html.
- R. Wang, H. Li, X. Han, Y. Zhang, and T. Baldwin. Learning from failure: Integrating negative examples when fine-tuning large language models as agents, 2024. URL https://arxiv.org/abs/2402.11651.
- J. Wei, X. Wang, D. Schuurmans, M. Bosma, brian ichter, F. Xia, E. H. Chi, Q. V. Le, and D. Zhou. Chain of thought prompting elicits reasoning in large language models. In A. H. Oh, A. Agarwal, D. Belgrave, and K. Cho, editors, *Advances in Neural Information Processing Systems*, 2022. URL https://openreview.net/forum?id=_VjQlMeSB_J.
- A. Yang, A. Li, B. Yang, B. Zhang, B. Hui, B. Zheng, B. Yu, C. Gao, C. Huang, C. Lv, C. Zheng, D. Liu, F. Zhou, F. Huang, F. Hu, H. Ge, H. Wei, H. Lin, J. Tang, J. Yang, J. Tu, J. Zhang, J. Yang, J. Zhou, J. Zhou, J. Lin, K. Dang, K. Bao, K. Yang, L. Yu, L. Deng, M. Li, M. Xue, M. Li, P. Zhang, P. Wang, Q. Zhu, R. Men, R. Gao, S. Liu, S. Luo, T. Li, T. Tang, W. Yin, X. Ren, X. Wang, X. Zhang, X. Ren, Y. Fan, Y. Su, Y. Zhang, Y. Zhang, Y. Wan, Y. Liu, Z. Wang, Z. Cui, Z. Zhang, Z. Zhou, and Z. Qiu. Qwen3 technical report, 2025. URL https://arxiv.org/abs/2505.09388.
- G. Yehudai and O. Shamir. On the power and limitations of random features for understanding neural networks. In H. Wallach, H. Larochelle, A. Beygelzimer, F. d'Alché-Buc, E. Fox, and R. Garnett, editors, *Advances in Neural Information Processing Systems*, volume 32. Curran Associates, Inc., 2019. URL https://proceedings.neurips.cc/paper_files/paper/2019/file/5481b2f34a74e427a2818014b8e103b0-Paper.pdf.
- M. Yuksekgonul, F. Bianchi, J. Boen, S. Liu, Z. Huang, C. Guestrin, and J. Zou. Textgrad: Automatic "differentiation" via text, 2024. URL https://arxiv.org/abs/2406.07496.

A ADDITIONAL EXPERIMENTAL DETAILS AND RESULTS

A.1 EVALUATION TASKS

We evaluate both methods across a diverse suite of algorithmic tasks designed to probe different facets of logical reasoning, from simple pattern recognition to complex, non-local computations. For each task, the training and test datasets are balanced with an equal number of positive and negative examples. (Add a footnote, for dimension 20 in Dyck-2 it is impossible to create sufficient positive labels, hence test set here is reduced to 1000 samples).

- Parity. Parity functions are functions of the form $(-1)^{\langle s,x\rangle}$, where $s\in\{0,1\}^n$ is a fixed binary vector. We experiment with multiple types of parity functions: the full parity function $(-1)^{\langle \mathbf{1}_n,x\rangle}$ (where $\mathbf{1}_n=(1,\ldots,1)$ of length n), the first-half parity function $(-1)^{\langle (\mathbf{1}_{n/2}\|\mathbf{0}_{n/2}),x\rangle}$ (where $(\mathbf{1}_{n/2}\|\mathbf{0}_{n/2})$ is the concatenation of $\mathbf{1}_{n/2}=(1,\ldots,1)$ and $\mathbf{0}_{n/2}=(0,\ldots,0)$), random k-parity, which is a function of the form $(-1)^{\langle s,x\rangle}$ with a random vector s with k 1s and n-k zeros.
- Pattern Matching. For a fixed pattern $p \in \{0,1\}^k$ with k < n, the label is $y(x) = \mathbb{I}[\exists i \in \{1,\ldots,n-k+1\}$ such that $(x_i,\ldots,x_{i+k-1})=p]$, where $\mathbb{I}[\cdot]$ is the indicator. We use patterns 10101010 and 001111111 to assess local feature detection.
- **IsPalindrome.** This function is defined as $y(x) = \mathbb{I}[\forall i \in \{1, \dots, \lfloor n/2 \rfloor\} : x_i = x_{n-i+1}]$. Positive examples (palindromes) are constructed by mirroring a random first half. For negatives, we generate a palindrome and flip a single bit in the first half, thereby testing sensitivity to precise symmetric structure.
- Dyck-2. Let $\mathcal{M}: \{0,1\}^2 \to \{`(`,`)`,`[`,`]`\}$ be a mapping from bit-pairs to characters, and let S(x) be the resulting character string. The function is $y(x) = \mathbb{I}[S(x) \in D_2]$, where D_2 is the Dyck-2 formal language. This task assesses the ability to recognize a context-free language, which requires stack-like, recursive reasoning.
- IsPrime. The input sequence $x=(x_1,\ldots,x_n)$ encodes a base-10 integer with digits $x_i\in\{0,\ldots,9\}$. The label is $y(x)=\mathbb{I}[\operatorname{IsPrime}(\operatorname{int}(x))]$. This task requires arithmetic and number-theoretic reasoning, posing a challenge for neural networks. The dataset comprises equal numbers of randomly sampled n-digit primes and n-digit non-primes, each drawn uniformly from its respective set.
- IsPrime (Ends in $\{1,3,7,9\}$). The function is unchanged, $y(x) = \mathbb{I}[\text{IsPrime}(\text{int}(x))]$, but the dataset is constrained so that the last digit $x_n \in \{1,3,7,9\}$. This removes the most common statistical shortcuts for primality and forces reliance on number-theoretic properties that depend on the entire sequence.
- Cellular Automaton Parity. The label is $y(x) = \left(\sum_{i=1}^n x_i'\right) \mod 2$, where $x' = (x_1', \dots, x_n')$ is derived from x by a local update. Each bit x_i' depends on its neighborhood (x_{i-1}, x_i, x_{i+1}) via $x_i' = x_{i-1} \oplus (x_i \vee x_{i+1})$. We use boundary conditions $x_0 = x_{n+1} = 0$. The task combines a local, nonlinear (and potentially chaotic) transform with a global parity computation.
- SHA-256 Parity. Let $(h_1, \ldots, h_{256}) = \text{SHA-256}(x)$ be the 256-bit hash of x. The label is $y(x) = \left(\sum_{i=1}^{256} h_i\right) \mod 2$. Because cryptographic hashes are effectively pseudorandom, this task is a stringent test of a model's ability to learn highly complex, nonlinear dependencies.

A.2 ADDITIONAL RESULTS

To test the robustness of our main result—that SGD fails to achieve algorithmic generalization—we ran ablations reported in the appendix: (i) training from scratch with different models (App. A.2.1, Tab. 2, Fig. 12) (ii) fine-tuning pretrained LLMs in place of training from scratch (App. A.2.2, Tab. 3, Fig. 13), (iii) in-context learning (App. A.2.3, Tab. 3, Fig. 14), (iv) length generalization (App. A.2.4, Tab. 4) (v) data scaling (App. A.2.5, Tab. 5 and 6) (vi) batch size (App. A.2.6, Tab. 7, Fig. 16) and (vii) learning rate (App. A.2.7, Tab. 8, Fig. 17). Across all settings, models fit the training data yet failed to achieve algorithmic generalization; this pattern persists over wide hyperparameter sweeps and with fine-tuning, indicating the effect is not an artifact of configuration choices but a limitation of SGD on these tasks.

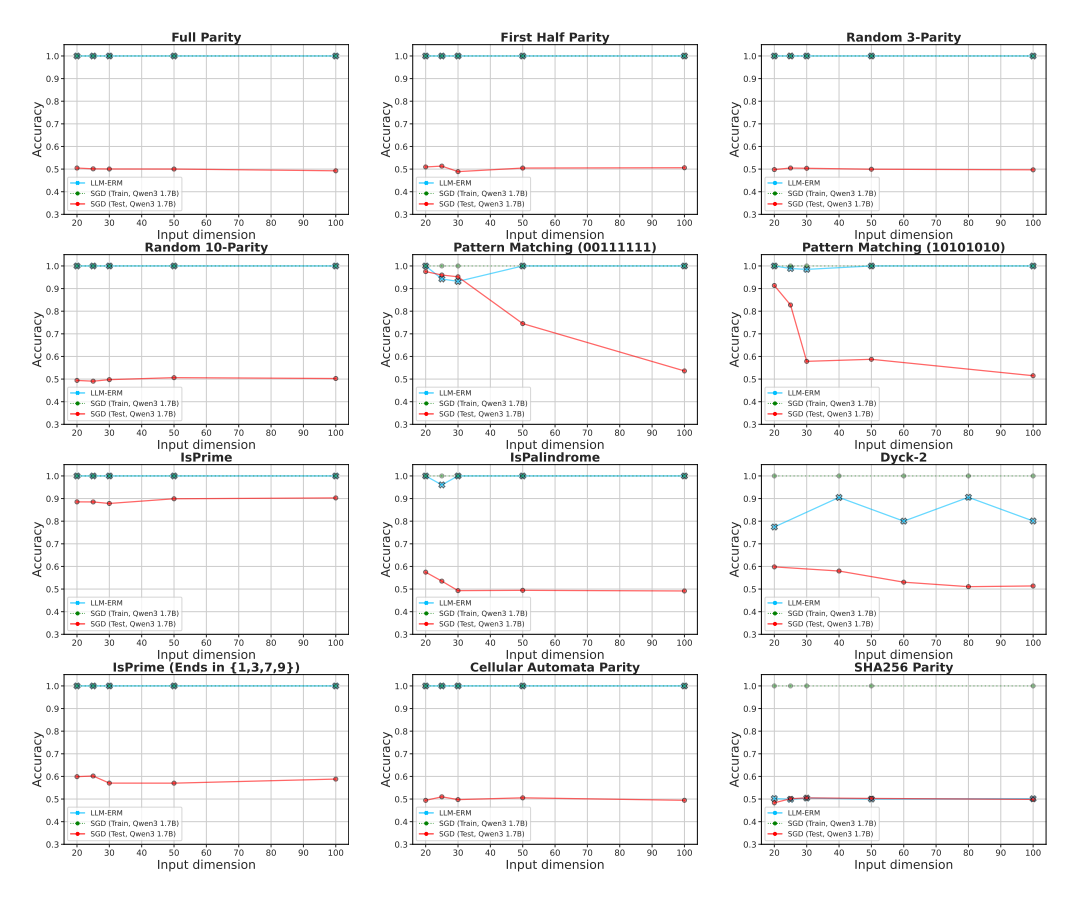


Figure 11: **LLM-ERM generalizes from 200 samples, while SGD-trained LLM overfits.** With only 200 training examples per task, LLM-ERM typically recovers the target function exactly, whereas SGD training of Qwen3-1.7B from scratch fits the training data but fails to generalize on most tasks when n is sufficiently large. Due to the extreme pseudo-random behavior of the SHA-256 function, it remains difficult to learn by both LLM-ERM and SGD.

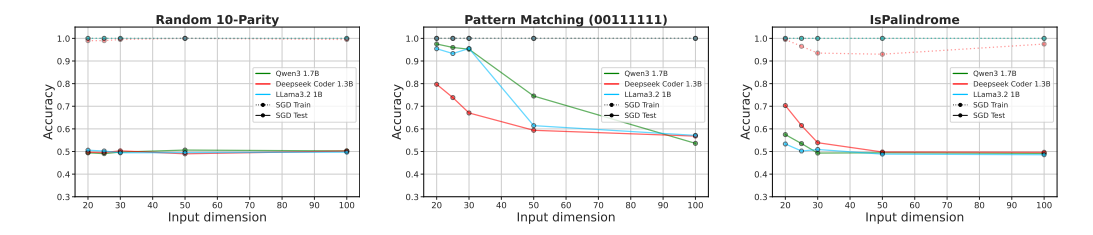


Figure 12: **Different LLM architectures consistently overfit the training data.** We compare architectures on three tasks—Random 10-Parity, Pattern Matching (00111111), and IsPalindrome. All models exhibit the same issue described above: they fit the training data but fail to generalize when the sequence length is too large.

A.2.1 TRAINING FROM SCRATCH

To complement the results in Fig. 5, we conducted similar experiments with all the tasks described in App. A.1. As can be seen in Fig. 11, our method achieves 100% test accuracy across all tasks and sequence lengths except for Dyck-2 and SHA-256.

To determine if the poor generalization was specific to the <code>Qwen3-1.7B</code> architecture, we replicated our SGD experiments with two other prominent open-source models of similar scale: <code>Deepseek-Coder-1.3B</code> and <code>Llama3.2-1B</code>. Each model was trained from scratch under identi-

		Qwen3-1.7B				Deepseek-Coder-1.3B				Llama3.2-1B					
Task	n=20	n=25	n = 30	n = 50	n = 100	n=20	n=25	n = 30	n = 50	n = 100	n=20	n=25	n = 30	n = 50	n = 100
Rand. 10-Parity	49.4%	49.1%	49.8%	50.6%	50.3%	49.7%	49.5%	50.3%	49.0%	50.2%	50.6%	50.2%	49.4%	49.5%	49.7%
Pattern Matching (00111111)	97.5%	96.0%	95.2%	74.5%	53.6%	79.7%	73.8%	67.0%	59.4%	56.8%	95.4%	93.3%	95.5%	61.4%	57.1%
IsPalindrome	57.5%	53.5%	49.3%	49.4%	49.2%	70.3%	61.5%	53.9%	49.8%	49.7%	53.3%	50.2%	50.9%	48.8%	48.6%

Table 2: **Test accuracy rates across different model architectures.** All models demonstrate failure on the Random 10-Parity task. For IsPalindrome and Pattern Matching, accuracy is high for shorter sequences but degrades significantly as sequence length increases.

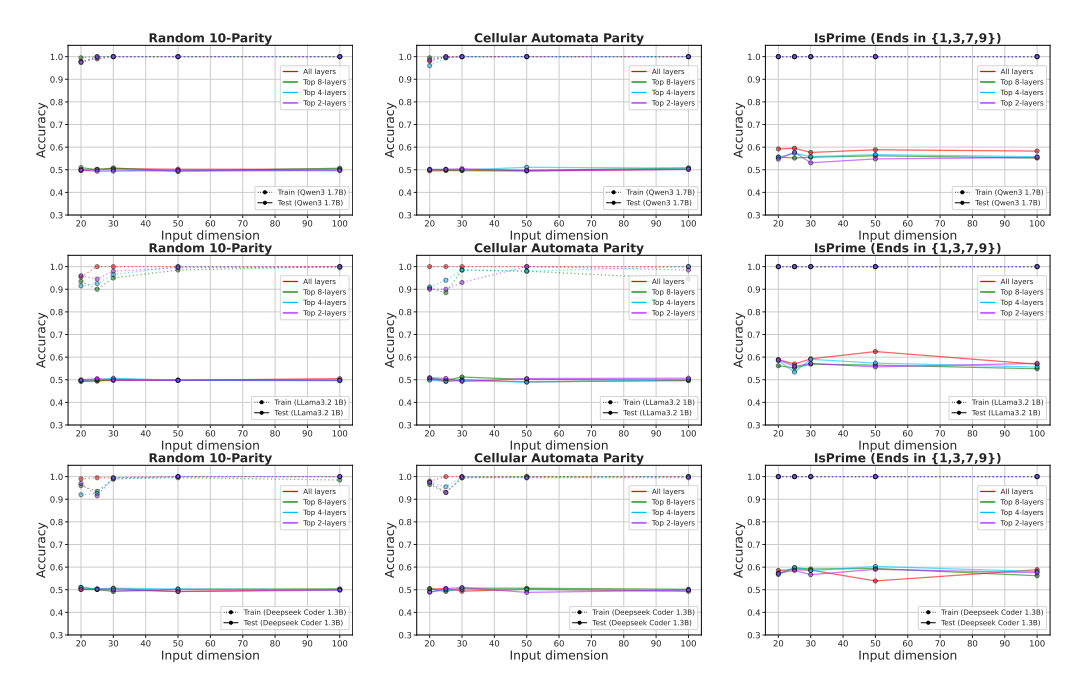


Figure 13: Fine-tuning pre-trained LLMs fails to overcome overfitting on algorithmic tasks. We fine-tuned Qwen3-1.7B, Llama3.2-1B, and Deepseek-Coder-1.3B on all tasks with 200 samples, training either the full model or only the top 2, 4, or 8 layers. While models could partially fit the data—or perfectly fit it when the full network was fine-tuned—their test accuracy remained near 50%.

cal conditions, using the same hyperparameters and training data as described in our main experiments. We evaluated them on a representative subset of tasks: IsPalindrome (non-local reasoning), Random 10-Parity (sparse non-local reasoning), and Pattern Matching (00111111) (heuristic-based reasoning).

As shown in Tab. 2 and Fig. 12, the choice of architecture had no significant impact on generalization performance. For Random 10-Parity, all three models: Qwen3-1.7B, Deepseek-Coder-1.3B, and Llama3.2-1B, performed at chance level on the test set (50% accuracy), confirming a consistent failure to learn sparse non-local dependencies. For IsPalindrome and Pattern Matching, the models achieved high accuracy on shorter sequences but failed to generalize as sequence length increased, with performance degrading significantly towards chance level. This consistency across architectures strongly suggests that the failure to generalize is a fundamental limitation of the SGD paradigm for these complex algorithmic tasks, where models learn shallow heuristics that do not scale with problem size, rather than a deficiency of a particular model.

A.2.2 FINE-TUNING PRE-TRAINED MODELS

We fine-tuned three pre-trained LLMs—Qwen3-1.7B Yang et al. (2025), Llama3.2-1B (Meta AI, 2024), and Deepseek-Coder-1.3B Guo et al. (2024)—on Random 10-Parity, Cellular Automata Parity, and IsPrime (restricted to numbers ending in $\{1,3,7,9\}$). Fine-tuning used 200 training samples and 10k test samples, with input lengths $n \in \{20,25,30,50,100\}$. Models were trained for 1000 epochs using the AdamW (Loshchilov and Hutter, 2019) optimizer with a CosineAnnealingLR scheduler (Loshchilov and Hutter, 2019). For each configuration of model

		I .				F	ine-Tunir	g Pre-tra	ined Mod	lels (Test	Accuracy)				
		i —	L	lama3.2-	1B				Qwen3-1.7	7B			Deepse	eek-Code	r-1.3B	
Task	Layers Tuned	n=20	n=25	n = 30	n = 50	n = 100	n=20	n=25	n=30	n = 50	n = 100	n=20	n=25	n = 30	n=50	n=100
	Top 2	50.0%	50.4%	49.8%	51.2%	50.0%	50.5%	51.0%	50.3%	49.2%	49.6%	49.8%	49.4%	50.0%	50.7%	50.1%
Full Parity	Top 4 Top 8	50.0% 49.7%	50.1% 49.7%	50.3% 50.4%	49.4% 50.2%	49.7% 50.3%	50.8% 50.3%	49.0% 48.9%	49.9% 49.9%	50.2% 49.9%	50.8% 51.2%	50.4% 49.1%	50.6% 50.5%	50.4% 49.5%	49.5% 50.1%	50.1% 50.5%
	Full Model	50.5%	50.3%	48.8%	49.7%	50.4%	50.7%	51.0%	49.6%	49.9%	49.8%	50.4%	49.7%	49.1%	50.7%	50.0%
	Top 2	52.7%	50.0%	50.6%	49.5%	50.6%	51.9%	51.3%	49.8%	50.5%	49.6%	52.3%	50.2%	50.6%	49.2%	50.2%
First Half Parity	Top 4	50.8%	49.5% 50.3%	49.9%	49.8%	49.8%	52.4%	50.4%	49.7% 50.4%	50.5% 49.8%	49.2% 49.9%	51.0%	50.9%	49.3%	50.1%	49.2%
	Top 8 Full Model	51.0% 49.2%	50.2%	50.8% 49.3%	49.6% 49.8%	51.3% 49.4%	52.3% 50.2%	50.1% 50.6%	50.4%	50.3%	50.7%	51.6% 49.1%	51.7% 49.3%	49.6% 49.6%	50.2% 50.0%	50.0% 50.1%
	Top 2	63.0%	65.7%	63.9%	68.5%	54.0%	71.9%	68.9%	66.6%	61.3%	56.3%	69.2%	66.2%	64.9%	58.5%	54.7%
Pattern Matching	Top 4	69.9%	63.8%	65.1%	60.2%	53.6%	74.5%	69.2%	66.1%	62.8%	58.5%	71.9%	66.9%	62.6%	56.2%	53.9%
(10101010)	Top 8 Full Model	70.0% 72.7%	64.6% 68.8%	63.9% 68.4%	57.8% 61.5%	54.8% 61.5%	70.2% 74.6%	69.1% 72.0 %	62.4% 66.1%	63.2% 64.8%	56.2% 59.6%	69.7% 70.9%	65.7% 67.8 %	63.8% 66.0%	58.8% 58.7%	56.4% 53.9%
	Top 2	66.7%	63.9%	61.4%	67.3%	57.6%	66.4%	64.0%	61.9%	61.1%	57.3%	67.0%	65.9%	60.8%	56.5%	57.7%
Pattern Matching	Top 4	62.9%	66.1%	59.7%	57.9%	55.5%	65.8%	62.4%	63.1%	60.5%	59.2%	64.9%	65.8%	62.5%	59.9%	56.8%
(00111111)	Top 8	66.4%	64.4%	63.2%	59.5%	55.0%	67.2%	64.6%	61.8%	62.6%	56.5%	65.4%	64.3%	61.0%	61.3%	56.0%
	Full Model	69.4%	63.5%	66.2%	65.7%	57.2%	65.5%	69.2%	67.4%	64.4%	59.4%	67.9%	64.6%	65.9%	62.4%	56.1%
	Top 2	48.6% 49.8%	50.7% 49.9%	50.7% 51.6%	50.7% 49.9%	51.0% 50.0%	50.3% 49.4%	50.3% 50.1%	50.9% 49.6%	50.1% 49.9%	50.5% 50.3%	50.0% 50.0%	50.3% 48.9%	51.3% 52.5%	50.2% 50.2%	50.2% 50.0%
Random 3-Parity	Top 4 Top 8	50.5%	50.4%	51.1%	50.4%	50.0%	50.9%	50.1%	50.5%	49.9%	49.7%	49.7%	48.9%	52.2%	50.2%	49.6%
	Full Model	50.9%	49.4%	51.6%	51.0%	50.1%	50.4%	50.1%	51.1%	50.1%	50.9%	50.2%	50.3%	53.3%	50.4%	50.7%
	Top 2	50.0%	50.5%	49.8%	49.8%	49.8%	49.9%	49.4%	49.4%	50.2%	49.6%	50.1%	50.1%	49.9%	49.2%	49.8%
Random 10-Parity	Top 4	49.7%	50.1%	50.7%	49.8%	49.6%	49.9%	50.1%	50.0%	49.3%	49.9%	51.0%	50.3%	50.7%	50.3%	50.0%
•	Top 8 Full Model	49.2% 49.7%	49.5% 49.5%	50.2% 49.7%	49.8% 49.8%	49.8% 50.5%	50.9% 49.6%	50.0% 50.2%	50.8% 50.5%	49.4% 50.2%	50.7% 50.2%	51.1% 50.1%	50.1% 50.3%	49.2% 50.5%	50.2% 49.2%	50.4% 50.1%
	Top 2	52.1%	49.7%	50.7%	49.7%	49.2%	52.0%	51.0%	50.6%	50.1%	49.6%	52.3%	49.4%	51.1%	49.3%	49.7%
IsPalindrome	Top 4	50.4%	47.6%	50.6%	49.5%	49.3%	51.8%	51.3%	50.6%	50.0%	49.2%	52.1%	50.1%	50.6%	49.2%	49.1%
isi amurome	Top 8	52.1%	49.6%	50.1%	50.2%	49.6%	52.4%	50.9%	50.6%	50.2%	49.0%	52.1%	49.8%	50.9%	50.1%	49.2%
	Full Model	51.0%	49.9%	50.4%	49.6%	49.0%	50.3%	49.7%	50.3%	49.6%	49.1%	50.4%	49.3%	49.6%	49.6%	49.1%
Dyck-2	Top 2 Top 4	54.5% 60.8%	55.7% 56.3 %	52.0% 52.1%	50.3% 49.5%	51.7% 52.7%	62.8% 64.1%	54.4% 53.5%	52.8% 53.6%	52.5% 51.6%	51.1% 51.2%	59.4% 60.7 %	53.1% 53.1%	51.9% 51.8%	50.7% 51.0%	50.0% 51.0%
	Top 8	61.5%	53.8%	53.1%	52.1%	49.8%	63.4%	53.7%	51.8%	52.1%	52.5%	60.4%	53.7%	52.0%	51.0%	51.7%
	Full Model	64.6%	53.8%	51.6%	50.7%	50.8%	62.7%	57.9%	51.3%	52.8%	50.8%	60.1%	54.4%	53.9%	51.6%	51.3%
	Top 2	57.4%	57.5%	57.6%	53.6%	58.4%	56.0%	55.2%	54.3%	54.5%	56.2%	58.4%	59.9%	58.0%	58.2%	59.7%
IsPrime	Top 4 Top 8	58.9% 55.8%	54.2% 57.5%	59.2% 59.9 %	56.0% 57.8%	58.8% 55.7%	58.7% 57.1%	55.3% 57.5%	55.8% 54.1%	55.6% 54.6%	56.0% 56.1%	54.5% 59.1 %	58.2% 57.7%	58.3% 58.1%	56.5% 58.2%	59.7% 54.2%
	Full Model	57.5%	61.7%	59.0%	56.5%	60.5%	60.3%	62.5%	59.4%	57.2%	59.3%	58.2%	59.6%	62.7%	61.1%	58.7%
	Top 2	58.8%	55.9%	57.2%	55.7%	57.2%	54.7%	57.8%	53.1%	54.8%	55.4%	57.3%	58.6%	56.7%	59.0%	57.6%
IsPrime	Top 4	58.5%	53.4%	59.0%	57.4%	55.6%	55.5%	57.3%	55.8%	56.7%	55.8%	56.7%	59.8%	58.4%	60.3%	58.0%
(Ends in {1,3,7,9})	Top 8 Full Model	56.2% 58.9%	55.2% 57.0 %	56.9% 59.2%	56.5% 62.5 %	54.9% 56.9%	55.6% 59.2%	55.2% 59.5 %	55.5% 57.7 %	56.2% 58.8%	55.2% 58.3%	57.2% 58.5%	59.6% 58.9%	59.2% 58.7%	59.4% 53.9%	56.2% 58.9%
	Top 2	50.9%	50.6%	49.3%	50.5%	50.7%	50.0%	50.2%	50.4%	49.6%	50.1%	48.9%	50.4%	51.0%	48.8%	49.8%
Cellular Automata	Top 4	49.8%	49.2%	49.7%	48.9%	50.1%	50.1%	50.2%	49.9%	51.1%	50.7%	49.1%	49.8%	50.1%	50.1%	49.8%
Parity	Top 8	50.8%	49.7%	51.2%	50.1%	49.9%	50.2%	50.0%	50.0%	49.7%	50.8%	50.5%	49.3%	50.7%	50.7%	50.2%
	Full Model	50.3%	49.4%	50.0%	49.1%	49.6%	49.5%	49.6%	49.6%	49.4%	50.2%	50.2%	50.6%	49.3%	50.2%	49.3%
	Top 2 Top 4	49.8% 50.0%	49.8% 49.7%	49.4% 49.8%	50.3% 48.8%	49.8% 50.8%	49.4% 50.7%	49.9% 50.3 %	49.4% 50.2%	49.5% 51.0%	49.5% 51.2%	50.3% 50.1%	50.5% 49.9%	49.6% 49.3%	50.6% 50.2%	49.7% 49.6%
SHA-256 Parity	Top 8	50.3%	50.1%	49.9%	49.7%	49.9%	49.4%	50.2%	49.0%	50.2%	50.1%	50.0%	49.1%	50.1%	50.2%	49.4%
	Full Model	49.3%	50.2%	50.8%	49.9%	50.1%	49.4%	49.2%	50.4%	50.7%	49.9%	50.1%	49.9%	50.1%	50.3%	49.7%
							In-C	ontext Le	arning (T	est Accur	acy)					
Task		1	Qwer	13-30B-In	struct			Qwen3-0	Coder-30I	3-Instruct	t	E	eepseek-	Coder-33	B-Instruc	t
		n=20	n=25	n=30	n=50	n=100	n=20	n=25	n=30	n=50	n=100	n=20	n=25	n=30	n=50	n=100
Full Parity		52.0%	43.0%	51.0%	38.0%	53.0%	49.0%	47.0%	47.0%	50.0%	50.0%	51.0%	47.0%	54.0%	51.0%	43.0%
First Half Parity	(40404040)	37.0%	49.0%	46.0%	59.0%	54.0%	50.0%	50.0%	46.0%	50.0%	50.0%	41.0%	45.0%	44.0%	52.0%	54.0%
Pattern Matching Pattern Matching		89.0% 79.0%	69.0% 68.0%	77.0% 63.0%	61.0% 79.0%	56.0% 51.0%	67.0% 77.0%	60.0% 66.0%	51.0% 72.0%	54.0% 51.0%	50.0% 50.0%	60.0% 59.0%	49.0% 45.0%	50.0% 48.0%	56.0% 53.0%	54.0% 47.0%
Random 3-Parity	(00111111)	54.0%	56.0%	51.0%	42.0%	50.0%	50.0%	50.0%	51.0%	44.0%	50.0%	44.0%	52.0%	48.0%	48.0%	47.0%
Random 10-Parity		45.0%	53.0%	54.0%	51.0%	50.0%	50.0%	49.0%	53.0%	42.0%	44.0%	51.0%	55.0%	55.0%	35.0%	48.0%
IsPalindrome		58.0%	48.0%	49.0%	49.0%	47.0%	52.0%	53.0%	51.0%	52.0%	51.0%	56.0%	47.0%	63.0%	47.0%	51.0%
Dyck-2 IsPrime		70.0% 57.0%	57.0% 62.0%	59.0% 56.0%	52.0% 66.0%	48.0% 52.0%	63.0% 59.0%	52.0% 55.0%	61.0% 53.0%	54.0% 51.0%	50.0% 49.0%	50.0% 47.0%	47.0% 57.0%	49.0% 45.0%	52.0% 47.0%	54.0% 57.0%
IsPrime (Ends in {		53.0%	53.0%	53.0%	57.0%	50.0%	52.0%	49.0%	50.0%	50.0%	47.0%	51.0%	49.0%	47.0%	53.0%	53.0%
Cellular Automata		47.0%	45.0%	44.0%	43.0%	49.0%	50.0%	47.0%	44.0%	49.0%	49.0%	52.0%	42.0%	46.0%	50.0%	44.0%
SHA-256 Parity		53.0%	48.0%	49.0%	51.0%	54.0%	48.0%	55.0%	51.0%	53.0%	49.0%	44.0%	46.0%	52.0%	53.0%	52.0%

Table 3: **Test accuracy for fine-tuning and in-context learning fails to generalize on algorithmic tasks.** (**Top**) Fine-tuning pre-trained models (1B scale) on 200 examples fails on non-local tasks (chance accuracy) and yields only marginal gains on heuristic-based ones, regardless of the number of layers tuned. (**Bottom**) In-context learning with larger instruction-tuned models (30B+ scale) and the same 200 examples also fails to generalize.

and input dimension, we determined the optimal hyperparameters via a grid search over batch sizes $\{20,50,100\}$ and learning rates $\{5\text{e-}3,1\text{e-}3,5\text{e-}4,1\text{e-}4,5\text{e-}5,1\text{e-}5\}$, selecting the configuration with the best training accuracy. This sweep identified a batch size of 20 as optimal for all models. The best-performing peak learning rates were 1×10^{-3} for Llama3.2-1B and 5×10^{-3} for Qwen3-1.7B and Deepseek-Coder-1.3B, with the scheduler annealing to a minimum rate of 1×10^{-3} . All training used bfloat16 precision, space-separated integer tokenization (EOS padding), and a single-logit LM head (hidden \rightarrow 1) at the final position.

In Fig. 13 and Tab. 3, we evaluated four different cases: fine-tuning the whole model and partial fine-tuning of only the top 2, 4, or 8 transformer blocks. Full fine-tuning typically achieved (near-)perfect training accuracy, while partial fine-tuning produced moderate fits. However, test

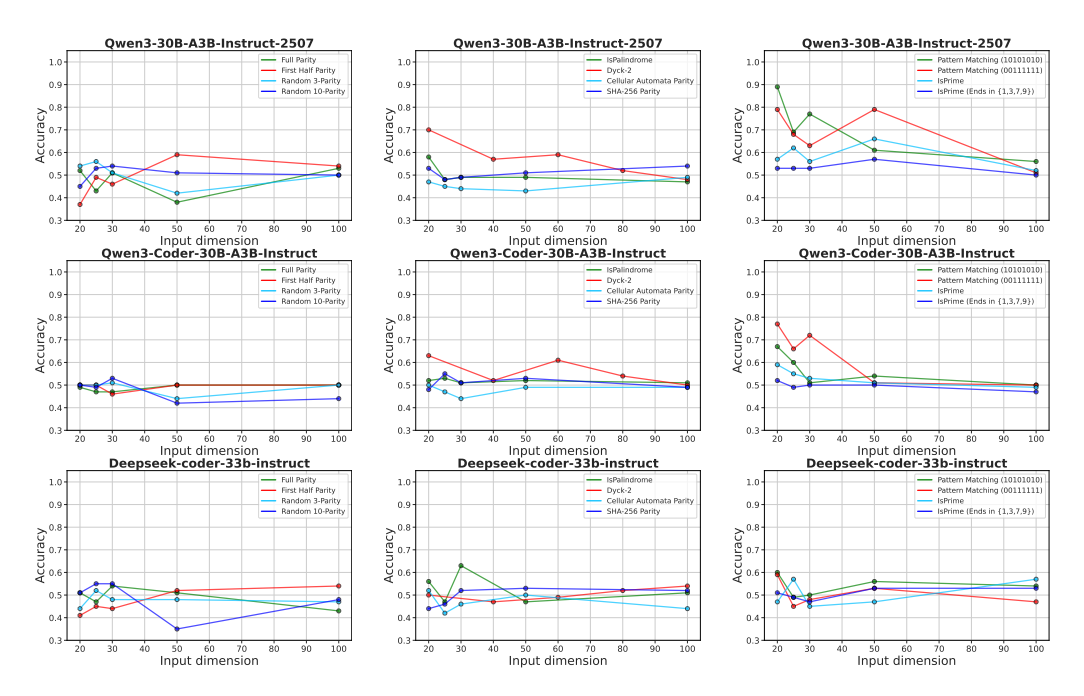


Figure 14: Test accuracy for in-context learning with three large models also fails to generalize. The plots display the performance of <code>Qwen3-30B-A3B-Instruct-2507(left)</code>, <code>Qwen3-Coder-30B-A3B-Instruct</code> (middle), and <code>Deepseek-Coder-33B-Instruct</code> (right) on classification tasks when provided with 200 training examples in-context. Results are shown for all tasks and three different models. The observed test accuracy remains near the 50% chance baseline across all tested sequence lengths, with the exception of Pattern Matching reaching up to 89.0% for n=20.

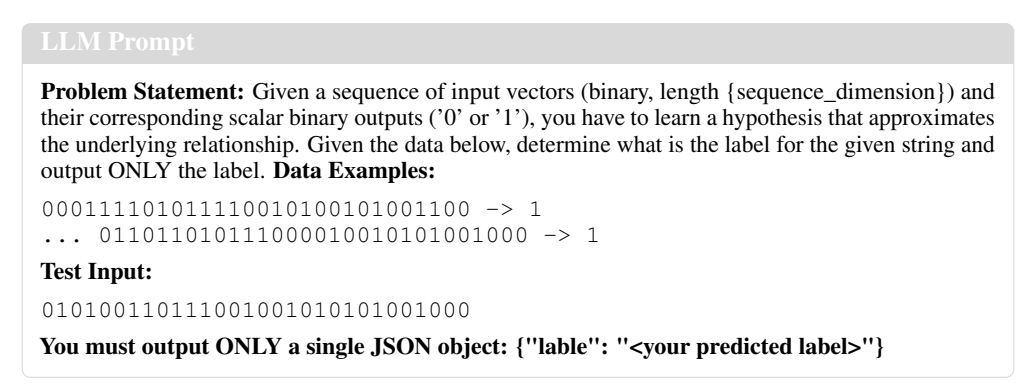


Figure 15: Prompt used in in-context learning procedure. We run three models Qwen3-30B-A3B-Instruct-2507, Qwen3-Coder-30B-A3B-Instruct, and Deepseek-Coder-33B-Instruct with this prompt. For each prompt, the model outputs only the predicted label for the test input.

performance remained essentially unchanged: on tasks requiring non-local dependencies (Random 10-Parity, Cellular Automata Parity), accuracy stayed at chance ($\approx 50\%$) across models, lengths, and depths. Notably, fine-tuning showed partial generalization on Pattern Matching reaching up to 74.6%, Dyck-2 up to 64.6%, and IsPrime yielding more modest improvements (e.g., 62.7% for Deepseek-Coder-1.3B full FT). Overall, no model under any fine-tuning regime demonstrated robust generalization on either of these tasks.

		Train Acc.	Test Accuracy (by length n)									
Task	Model		n=10	n=20	n = 25	n = 30	n=50	n=100				
IsPalindrome	Qwen3-1.7B	100%	98.2%	54.8%	46.9%	50.2%	49.9%	50.0%				
	LLM-ERM	100%	100%	100%	49.2%	70.3%	69.7%	69.6%				
Pattern Matching	Qwen3-1.7B	100%	98.6%	55.7%	52.5%	51.3%	50.2%	50.0%				
	LLM-ERM	100%	100%	100%	100%	100%	100%	100%				
Random 3-Parity	Qwen3-1.7B	99.5%	58.4%	55.2%	53.9%	53.1%	50.8%	50.2%				
	LLM-ERM	100%	100%	100%	100%	100%	100%	100%				

Table 4: **LLM-ERM exhibits length generalization, whereas the baseline overfits to input length.** Models were trained only at a fixed input length (n=10) and tested on longer, unseen sequences. The baseline attains near-perfect accuracy on the training data but fails to generalize, with performance collapsing to the $\approx 50\%$ chance level as n grows. In contrast, LLM-ERM synthesizes dimension-invariant programs for Pattern Matching and Random 3-Parity, achieving perfect generalization. For IsPalindrome, it generalizes better than the baseline but is not perfectly robust to length changes.

A.2.3 IN-CONTEXT LEARNING

An alternative to fine-tuning for adapting a pre-trained model is in-context learning (ICL). This experiment investigates whether a large, pre-trained LLM can infer the underlying function from examples provided directly in its context window and then apply that inferred rule to classify a new input. Formally, we test if the model's predictive function, $h(x_{\text{test}}|S_{\text{tr}})$, can approximate the target function $y(x_{\text{test}})$, where the training set S_{tr} (200 samples) is provided as context.

For this evaluation, we employed three large-scale, instruction-tuned models: Qwen3-30B-A3B-Instruct-2507 (Yang et al., 2025), Qwen3-Coder-30B-A3B-Instruct (Yang et al., 2025), and Deepseek-Coder-33B-Instruct (Guo et al., 2024). For each of the 100 test samples, a prompt Fig. 15 was constructed containing the problem statement, all 200 training examples, and a single test input, asking the model to predict the corresponding label. Generation was performed with deterministic settings to encourage logical reasoning (temperature of 0.2, top-p of 0.95) and a maximum of 1024 new tokens.

The results show that in-context learning fails to solve these algorithmic tasks. As detailed in the lower half of Tab. 3 and Fig. 14, test accuracy across nearly all tasks and sequence lengths remains near the 50% chance level, consistently across all three large models tested. A few tasks are notable exceptions: Pattern Matching reaches up to 89.0%, Dyck-2 reaches 70.0%, and IsPrime shows a modest improvement to 66.0% at test time.

A.2.4 LENGTH GENERALIZATION

To assess out-of-distribution generalization, we trained models exclusively on a dataset of 200 samples at a fixed input length of n=10. The resulting models were then evaluated on unseen test sets featuring longer sequences ($n \in \{10, 20, 25, 30, 50, 100\}$). For the SGD baseline, all other training hyperparameters, including the optimizer, learning rate scheduler, and number of epochs, remained identical to those used in our primary experiments to ensure a controlled comparison.

The results, detailed in Fig. 10 and Tab. 4, reveal a stark divergence in generalization. The SGD baseline is incapable of generalizing across the training dimension. Despite achieving 100% train accuracy and relatively high test accuracy on the $n{=}10$ data, its performance collapses to the $\approx 50\%$ chance level on all longer sequences. In contrast, LLM-ERM demonstrates robust length generalization by synthesizing dimension-invariant programs on Pattern Matching and Random 3-Parity. This ability is consistent with our primary findings in Tab. 1: for all parity variants, IsPrime (both variants), several Pattern Matching, and Cellular Automata Parity instances, LLM-ERM discovers functionally correct solutions that operate independently of input length, yielding perfect ($\infty\%$) test accuracy.

	BLOOM-75M											
Task	n = 20	n=25	n = 30	n = 50	n = 100							
Rand. 10-Parity	53.9%	49.8%	50.5%	49.2%	50.7%							
Cellular Automata Parity	99.9%	50.3%	50.2%	49.5%	50.4%							
IsPrime (Ends in {1,3,7,9})	59.8%	58.7%	60.3%	60.1%	59.9%							

Table 5: **Test accuracy** (%) **for BLOOM-75M trained on 100k examples per task.** Despite substantially more data, the model overfits and fails to achieve algorithmic generalization: performance is near chance on Random 10-Parity and Cellular Automata Parity across lengths, and only modest on ISPRIME with restricted negatives.

						Accu	racy vs. T	Training	Set Size				
		10	10k	100	10k	200	10k	1,000	10k	10,000	10k	100,000	10k
Task	Model	Train	Test	Train	Test	Train	Test	Train	Test	Train	Test	Train	Test
Random 10-Parity	BLOOM-75M LLM-ERM	100% 100%	49.9% 49.3%	100% 100%	49.1% 100%	100% 100%	49.7% 100%	100%	49.9% -	99.9%	50.1%	99.8%	50.7%
IsPrime (Ends in {1,3,7,9})	BLOOM-75M LLM-ERM	100% 100%	50.9% 50.5%	100% 100%	50.2% 100%	100% 100%	51.3% 100%	100%	56.4% -	100%	59.7% -	100%	59.9% -
Cellular Automata Parity	BLOOM-75M LLM-ERM	100% 100%	50.1% 50.3%	100% 100%	50.4% 50.1%	100% 100%	50.4% 100%	100%	50.0%	99.6%	50.0%	99.9%	50.4%

Table 6: A baseline LLM fails to generalize even with 100k samples, whereas LLM-ERM succeeds with only a few hundred samples. The SGD-trained BLOOM-75M model consistently overfits, achieving perfect training accuracy but failing to generalize beyond chance-level performance, even as the training set grows to 100k examples for n=100. In contrast, LLM-ERM demonstrates extreme sample-efficiency, finding correct programs for Random 10-Parity and IsPrime with as few as 100 samples and solving all three tasks with 200 samples. For LLM-ERM, the available samples were split equally for prompt generation and validation.

A.2.5 DATA SCALING

To investigate the impact of training set size on generalization, we trained the BLOOM-75M baseline using SGD across multiple data scales, using $m_{\rm train} \in \{10, 100, 200, 1000, 10k, 100k\}$ for $n{=}100$. This evaluation was conducted on Random 10-Parity, Cellular Automata Parity, and IsPrime (with restricted negatives). The BLOOM-75M model was trained for 1000 epochs and a constant learning rate of $\eta{=}10^{-5}$. The batch size was set to 256 for training sets with 1000 or more samples, and to 10 for smaller datasets. The model trained on this largest dataset was also evaluated across multiple input lengths $n \in \{20, 25, 30, 50, 100\}$.

The results highlight a failure of the SGD baseline to generalize, even with extensive data. As detailed in Fig. 7 and Tab. 6, increasing the training set size did not yield better test performance; the model consistently overfits, achieving perfect training accuracy while its test accuracy on Random 10-Parity and Cellular Automata Parity remained at the $\approx 50\%$ chance level. Furthermore, Fig. 6 and Tab. 5 show that even with 100k training samples, the model still overfits when the input dimension is too high, with performance again collapsing to chance. In contrast, LLM-ERM seems to be sample-efficient, synthesizing correct programs for all three tasks with a training set size of just 100-200.

A.2.6 BATCH SIZE

To assess the role of optimization dynamics, we ran a batch-size ablation with 200 training samples and batch sizes of 10, 20, 50, 100, and 200, holding all other hyperparameters fixed.

As shown in Tab. 7 and Fig. 16, generalization is only weakly affected by batch size. Random 10-Parity stays at chance across all settings, while the performance on IsPalindrome and Pattern Matching vary modestly by task. Most importantly, for each task and every batch size, generalization declines sharply as sequence length grows. This suggests the core behavior—memorizing complex patterns while failing to generalize cannot be easily solved by tuning the batch size.

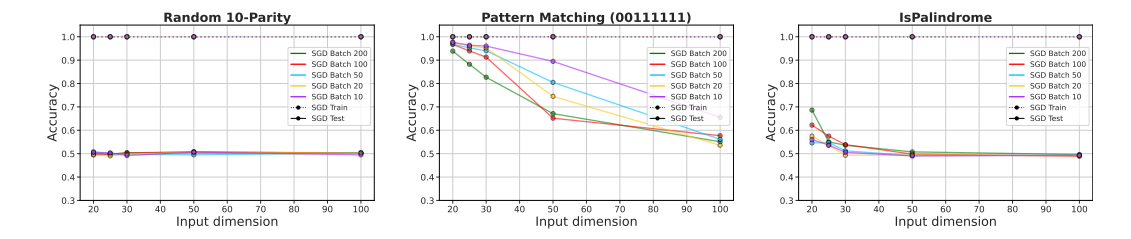


Figure 16: Varying the batch size does not resolve overfitting. We train instances of <code>Qwen3-1.7B</code> on Random 10-Parity (left), Pattern Matching (00111111) (middle), and IsPalindrome (right), reporting train and test accuracy. Changing the batch size does not materially alter the models' tendency to overfit.

Task	Batch Size	n = 20	n=25	n = 30	n = 50	n=100
Random 10-Parity	10	50.6%	50.4%	49.2%	50.7%	49.5%
·	20	49.4%	49.1%	49.8%	50.6%	50.3%
	50	50.8%	50.0%	49.7%	49.5%	50.3%
	100	49.6%	49.7%	50.3%	50.9%	50.2%
	200	50.1%	49.8%	50.4%	50.3%	50.4%
Pattern Matching (00111111)	10	97.7%	96.4%	96.0%	89.5%	65.5%
	20	97.5%	96.0%	95.2%	74.5%	53.6%
	50	96.9%	95.2%	94.0%	80.5%	56.1%
	100	96.7%	94.0%	91.3%	65.2%	57.7%
	200	93.8%	88.2%	82.7%	67.1%	55.1%
IsPalindrome	10	56.0%	53.7%	50.6%	49.0%	49.3%
	20	57.5%	53.5%	49.3%	49.4%	49.2%
	50	54.6%	54.8%	51.2%	49.2%	49.3%
	100	62.2%	57.5%	53.9%	49.8%	48.9%
	200	68.6%	55.0%	53.6%	50.8%	49.6%

Table 7: Accuracy is far more sensitive to sequence length than to batch size. Random 10-Parity stays at chance level across all configurations. Pattern Matching achieves high accuracy on short sequences but performance drops sharply as the sequences grow longer, regardless of batch size. For IsPalindrome, larger batches provide some benefit on shorter sequences, but accuracy still declines toward chance-level on longer ones.

A.2.7 LEARNING RATE

The learning rate is a critical factor in model convergence and generalization. To examine whether the poor generalization of SGD on the proposed program learning tasks is due to learning-rate choice, we conducted an ablation study. Specifically, we performed a comprehensive sweep across seven orders of magnitude, from 8.0 down to 8×10^{-7} . We evaluated Qwen3-1.7B on three representative tasks—Random 10-Parity, Pattern Matching (00111111), and IsPalindrome. Each model was trained for 200 epochs with batch size 20 on 200 training samples and evaluated on 10k random test samples.

As shown in Tab. 8 and Fig. 17, the effect of the learning rate varies substantially across tasks. For Random 10-Parity, generalization failure is insensitive to η : test accuracy remains near 50% across the entire sweep, indicating that no learning rate enables generalization. In contrast, IsPalindrome and Pattern Matching exhibit strong sensitivity to η . Pattern Matching can be solved perfectly for short sequences (n=20), but this success is brittle and does not extend to longer inputs. Similarly, IsPalindrome shows modest generalization for small n only at very low learning rates. For these more complex tasks, no broad optimal range exists; performance is highly sensitive, and effective generalization remains weak, particularly for longer sequences.

Task	Learning Rate (η)	n=20	n = 25	n=30	n=50	n=100
	8×10^{0}	50.0%	50.0%	50.0%	50.0%	50.0%
	8×10^{-1}	50.0%	50.0%	50.0%	50.0%	50.0%
	8×10^{-2}	50.0%	50.0%	50.0%	50.0%	50.0%
Random 10-Parity	8×10^{-3}	50.0%	50.0%	50.0%	50.0%	50.0%
Kandom 10-1 arity	8×10^{-4}	49.3%	51.0%	50.4%	50.2%	50.4%
	8×10^{-5}	50.4%	49.1%	50.2%	50.0%	51.1%
	8×10^{-6}	49.9%	50.3%	49.9%	49.0%	50.2%
	8×10^{-7}	50.2%	50.1%	49.8%	49.9%	50.1%
	8×10^{0}	50.0%	50.0%	50.0%	50.0%	50.0%
	8×10^{-1}	50.0%	58.7%	50.0%	50.0%	50.0%
	8×10^{-2}	50.0%	50.0%	50.0%	50.0%	50.0%
Pattern Matching	8×10^{-3}	95.7%	50.0%	50.0%	57.2%	56.5%
(00111111)	8×10^{-4}	95.2%	94.5%	93.9%	73.5%	53.5%
	8×10^{-5}	100.0%	94.8%	91.8%	87.9%	56.5%
	8×10^{-6}	95.7%	92.7%	84.2%	72.2%	56.9%
	8×10^{-7}	83.8%	78.6%	71.5%	57.6%	56.8%
	8×10^{0}	50.0%	53.8%	50.0%	50.0%	50.0%
	8×10^{-1}	50.0%	53.9%	50.0%	50.0%	50.0%
	8×10^{-2}	50.0%	46.4%	50.0%	50.0%	50.0%
IsPalindrome	8×10^{-3}	50.0%	54.2%	49.6%	50.0%	50.0%
isi ailiui viile	8×10^{-4}	53.9%	51.9%	49.8%	49.1%	49.4%
	8×10^{-5}	55.4%	53.6%	52.4%	49.0%	49.1%
	8×10^{-6}	67.5%	60.5%	51.3%	50.3%	49.2%
	8×10^{-7}	72.4%	60.2%	54.5%	49.9%	49.0%

Table 8: Test accuracy across a wide range of learning rates (η) . The model's inability to generalize on Parity tasks persists regardless of η . Pattern Matching and IsPalindrome learns for shorter sequence lengths but accuracy degrades on longer sequence lengths.

A.3 LLM REASONING TRACES

We extend the reasoning-trace analysis from Fig. 1 to the Cellular Automata Parity and Full Parity tasks, in order to further reveal the model's adaptive problem-solving strategies.

For the more complex Cellular Automata Parity task (Fig. 18), the reasoning trace initially mirrors the approach observed for Random 10-Parity (Fig. 1b). The model begins by testing simple batch statistics and basic parity checks, then searches for a linear solution. When no straightforward rule emerges, it escalates to systematically exploring a richer feature space of non-linear combinations. This includes testing thresholds and computing the parity of masked compositions that involve diverse features such as the first and last bits, a majority-ones flag, the parity of bit flips, and the parity of specific bigrams ("01", "10", etc.). This exhaustive exploration eventually produces the correct, more complex hypothesis. Finally, the model attempts a simplification step before converging on and confirming this solution, indicating a form of internal verification.

In stark contrast, when presented with the Full Parity task, the model's reasoning is immediate and conclusive. As shown in Fig. 19, it quickly dismisses simple heuristics such as ones-count thresholding, then immediately proposes the exact full-parity function over all bits. The hypothesis is tested against the dataset, achieves perfect alignment with the labels, and is subsequently verified without the need for extended exploration.

Unlike the Cellular Automata Parity case, where the model incrementally explores a large feature space of non-linear candidates, here the solution emerges almost instantly and is verified in a single step, highlighting the model's ability to identify and lock onto the correct global rule when it is especially simple.

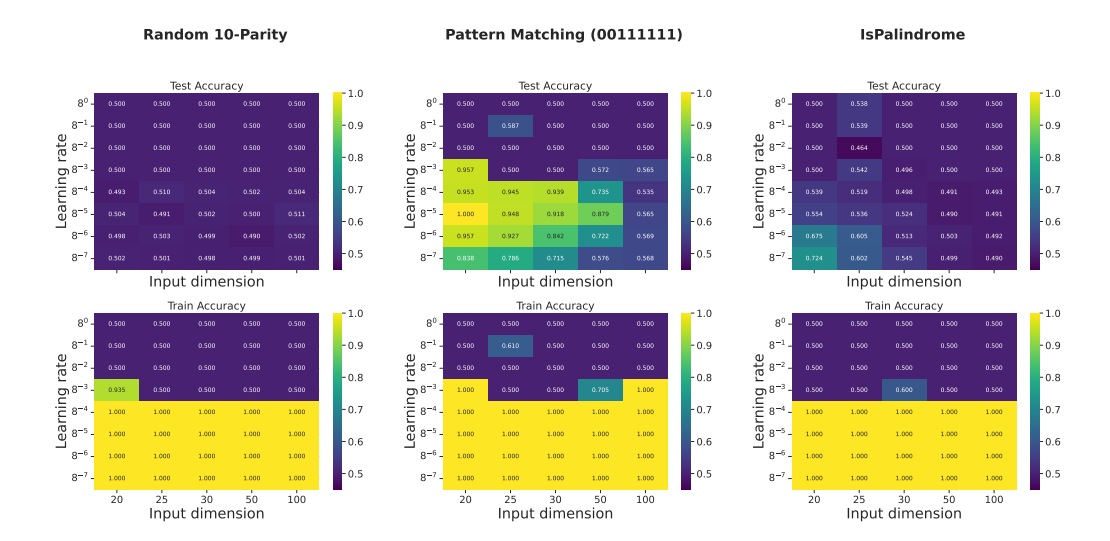


Figure 17: **SGD's failure to generalize is not due to poor learning-rate choices.** We trained Qwen3-1.7B for 200 epochs (batch size 20) with learning rates η swept across seven orders of magnitude, reporting train and test accuracy as sequence length n varies. Results are shown for Random 10-Parity (**left**), Pattern Matching (00111111) (**middle**), and IsPalindrome (**right**). For Random 10-Parity, test accuracy remains at chance ($\approx 50\%$) regardless of η , indicating no learning rate yields generalization. For Pattern Matching and IsPalindrome, certain η values succeed on short sequences (n=20) but fail to generalize as n increases.

Algorithm 2 Length-First Program Search (LFPS)

```
Require: Sample S = \{(x_i, y_i)\}_{i=1}^m, language \mathcal{L} \subseteq \Sigma^*, per-run timeout T \in \mathbb{N}, optional max
     length L_{\max} \in \mathbb{N} \cup \{\infty\}
Ensure: A program u^* \in \mathcal{L} whose total semantics [\![u^*]\!]: \mathcal{X} \to \{\pm 1\} satisfies [\![u^*]\!](x_i) = y_i for all
     (x_i, y_i) \in S; or \perp if none is found up to L_{\max}
 1: for \ell = 1, 2, ..., L_{\max} do
        for all strings u \in \mathcal{L} with |u| = \ell in lexicographic order do
           if u fails to compile then continue
 3:
 4:
           consistent \leftarrow true
 5:
           for each (x_i, y_i) \in S do
              Run u on input x_i for at most T steps; let o_i \in \{\pm 1, \bot\} be the output (\bot if no halt)
 6:
 7:
              if o_i = \bot or o_i \neq y_i then
 8:
                 consistent \leftarrow false; break
 9:
              end if
           end for
10:
           if consistent then
11:
              return u^{\star} \leftarrow u
                                                                              {minimal-length consistent program}
12:
13:
           end if
14:
        end for
15: end for
16: return ⊥
                                                                 {no consistent total program found up to L_{\text{max}}}
```

B PROOFS

Theorem 1 (Valiant (1984); see also Cor. 2.3 of Shalev-Shwartz and Ben-David (2014)). Let $y: \mathcal{X} \to \{\pm 1\}$ be an unknown target function and let $\mathcal{H} \subset \{\pm 1\}^{\mathcal{X}}$ be a finite hypothesis class. Suppose we are in the realizable setting (i.e., $y \in \mathcal{H}$). Let $S = \{(x_i, y(x_i))\}_{i=1}^m$ be m training examples drawn i.i.d. from a distribution D over $\mathcal{X} \times \{\pm 1\}$. Then, with probability at least $1 - \delta$ over the draw of S, every hypothesis $h \in \mathcal{H}$ that is consistent with S satisfies

$$\operatorname{err}_D(h) \leq \frac{\log(|\mathcal{H}|) + \log(1/\delta)}{m}.$$

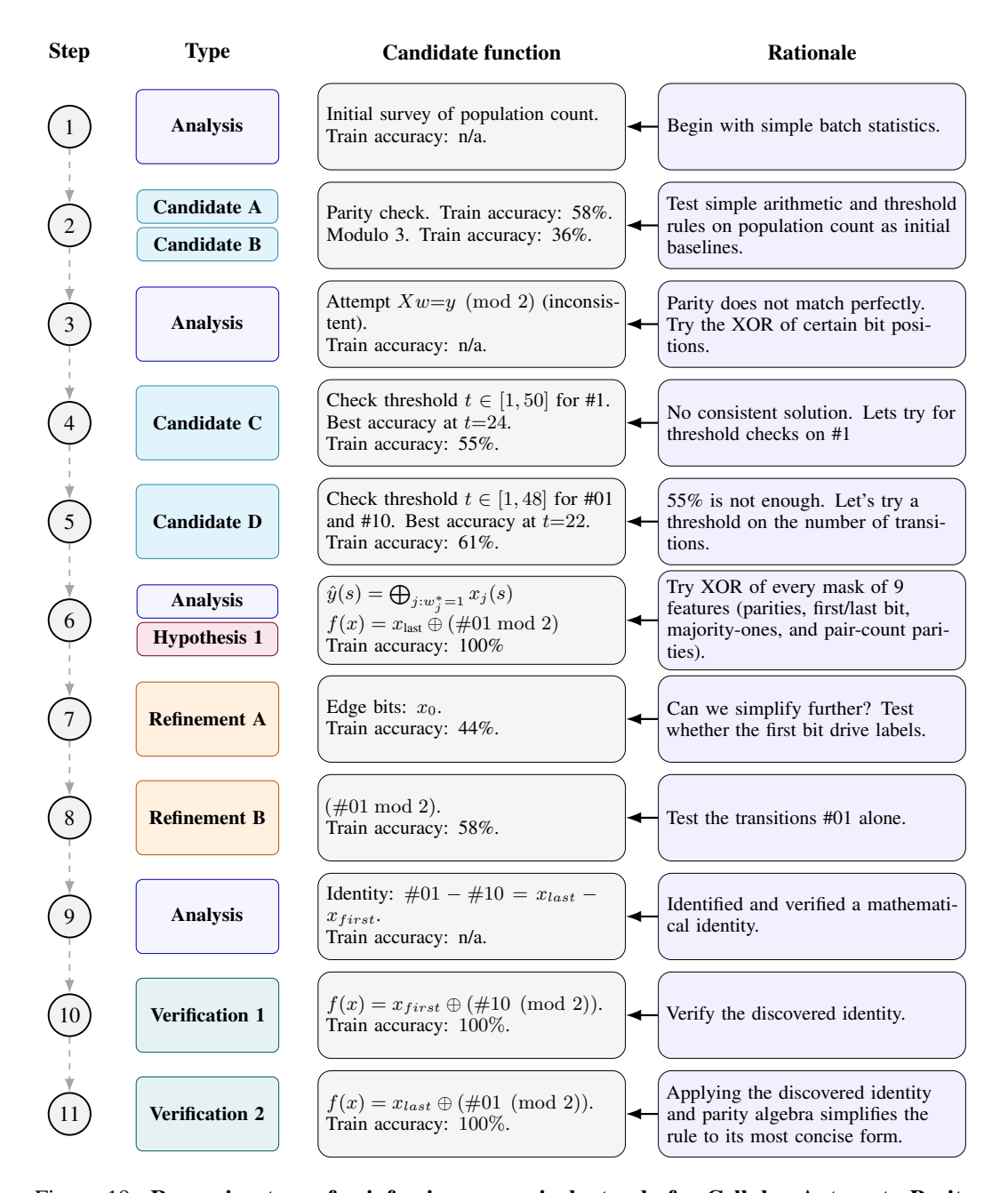


Figure 18: Reasoning trace for inferring an equivalent rule for Cellular Automata Parity function. The model starts with simple heuristics, explores linear solutions over \mathbb{F}_2 , and converges to a global XOR rule that perfectly matches the provided dataset, effectively inferring a simpler, equivalent function.

Corollary 1. Let $y: \mathcal{X} \to \{\pm 1\}$ be an unknown target function and let $\mathcal{H} = \bigcup_{\ell \geq 1} \mathcal{H}_{\ell} \subset \{\pm 1\}^{\mathcal{X}}$ be a union of finite sets. Suppose we are in the realizable setting (i.e., $y \in \mathcal{H}$). Let $S = \{(x_i, y(x_i))\}_{i=1}^m$ be m training examples drawn i.i.d. from a distribution D over $\mathcal{X} \times \{\pm 1\}$. Then, with probability at least $1 - \delta$ over the draw of S, for any $\ell \in \mathbb{N}$ and any hypothesis $h \in \mathcal{H}_{\ell}$ that is consistent with S, it holds that

$$\operatorname{err}_D(h) \leq \frac{\log(|\mathcal{H}_\ell|) + \log((\pi^2/6)\ell^2/\delta)}{m}.$$

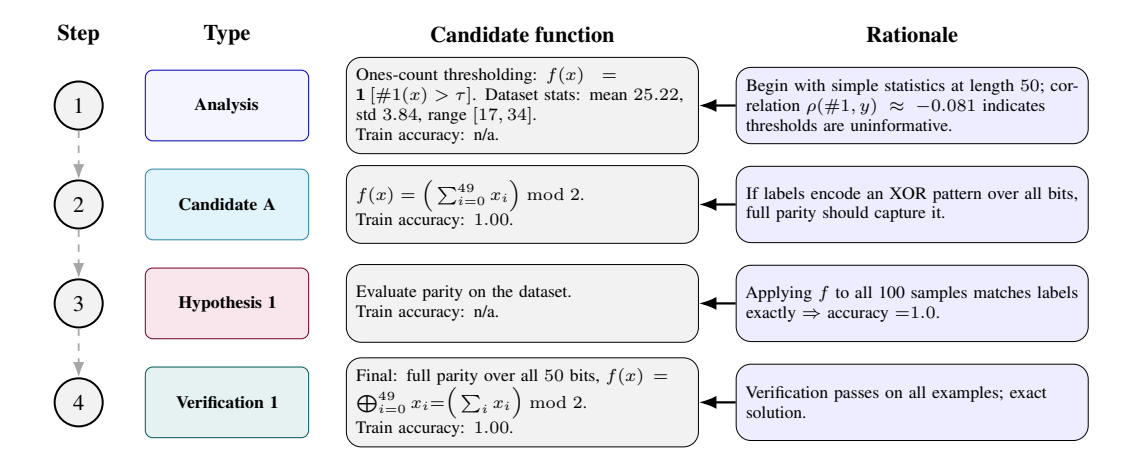


Figure 19: **Reasoning trace for learning a full-parity function.** We list the candidate functions proposed by GPT-5-thinking when trained on 100 binary strings of length 50. (**left**) The sequence of candidates explored. (**right**) The rationale for proposing each candidate. The model starts with simple statistics, hypothesizes full parity, and verifies that parity perfectly matches all labels.

Proof. Assume that $y \in \mathcal{H} = \bigcup_{\ell \geq 1} \mathcal{H}_{\ell}$; hence, there exists some ℓ^* for which \mathcal{H}_{ℓ^*} is realizable. For each fixed ℓ with at least one hypothesis consistent with S, Thm. 1 implies that for any $\delta_{\ell} > 0$, with probability at least $1 - \delta_{\ell}$, every $h \in \mathcal{H}_{\ell}$ consistent with S satisfies

$$\operatorname{err}_D(h) \leq \frac{\log(|\mathcal{H}_\ell|) + \log(1/\delta_\ell)}{m}.$$

Choose $\delta_\ell = \frac{6}{\pi^2} \frac{\delta}{\ell^2}$, so that $\sum_{\ell \geq 1} \delta_\ell = \delta$. Then, for each such ℓ , with probability at least $1 - \delta_\ell$,

$$\operatorname{err}_D(h) \ \leq \ \frac{\log(|\mathcal{H}_\ell|) + \log\left((\pi^2/6)\,\ell^2/\delta\right)}{m}.$$

Applying a union bound over all $\ell \geq 1$ yields the claim (for each ℓ with no consistent hypothesis, the inequality is vacuous).

Proposition 3. Suppose we wish to learn a target function $y: \mathcal{X} \to \{\pm 1\}$ that can be implemented as a program of length L in a programming language \mathcal{L} . Let \mathcal{L}_{ℓ} denote the set of programs of length ℓ in \mathcal{L} , and let $S = \{(x_i, y(x_i))\}_{i=1}^m$ be m training examples drawn i.i.d. from a distribution D over $\mathcal{X} \times \{\pm 1\}$. Then, with probability at least $1 - \delta$ over the draw of S, Alg. 2 outputs a program $h \in \mathcal{L}$ that is consistent with S and satisfies

$$\operatorname{err}_D(h) \leq \frac{L \log |\Sigma| + \log(2L^2/\delta)}{m}.$$

Proof. Since $y \in \mathcal{L}$, there exists a minimal length L such that $y \in \mathcal{L}_L$. Therefore, there is at least one program of length L consistent with S. Alg. 2 enumerates programs in order of increasing length, so it eventually returns a program h of some length $\ell \leq L$ that is consistent with S. Every program in \mathcal{L}_ℓ is described over the alphabet Σ , hence $|\mathcal{L}_\ell| \leq |\Sigma|^\ell$ and $\log |\mathcal{L}_\ell| \leq \ell \log |\Sigma| \leq L \log |\Sigma|$. Applying Cor. 1 with $\mathcal{H} = \mathcal{L}$ and $\mathcal{H}_\ell = \mathcal{L}_\ell$ and then upper-bounding by L gives

$$\operatorname{err}_D(h) \ \leq \ \frac{\log |\mathcal{L}_\ell| + \log(2\ell^2/\delta)}{m} \ \leq \ \frac{L\log |\Sigma| + \log(2L^2/\delta)}{m}.$$

B.1 FROM MINI-BATCH SGD TO 1-STAT(B) TO VSTAT: A FORMAL REDUCTION

Throughout, err_D denotes the 0–1 error. All query functions are measurable and bounded.

B.2 ORACLE MODELS

Definition 2 (1-STAT and 1-STAT(b)). Let D be a distribution over $\mathcal{X} \times \{\pm 1\}$. A 1-STAT oracle takes a Boolean function $g: \mathcal{X} \times \{\pm 1\} \to \{0,1\}$, draws a fresh $(x,y) \sim D$, and returns g(x,y). For $b \in \mathbb{N}$, a 1-STAT(b) oracle takes a vector of Boolean functions $g = (g_1, \ldots, g_b)$ and returns the b-bit vector $(g_1(x,y), \ldots, g_b(x,y))$ for a fresh $(x,y) \sim D$.

Definition 3 (VSTAT (Feldman, 2017, Definition 2.3)). Let D be as above. A VSTAT(t) oracle takes $g: \mathcal{X} \times \{\pm 1\} \to [0,1]$ and returns a value $v \in \mathbb{R}$ such that, writing $p = \mathbb{E}_D[g(x,y)]$,

$$|v-p| \le \max \left\{ \frac{1}{t}, \sqrt{\frac{p(1-p)}{t}} \right\}.$$

(The choice of v within the interval is adversarial; the interval width scales like the standard deviation of t i.i.d. samples.)

B.3 SIMULATING MINI-BATCH SGD USING 1-STAT(B)

Proposition 4 (SGD \Rightarrow 1-STAT(b)). Assume per-example coordinate gradients are uniformly bounded:

$$|\partial_j \ell(h_\theta, (x, y))| \le G$$
 for all $\theta, j, (x, y)$.

At iteration t, define

$$\phi_t(x,y) := \frac{1}{2} \left(1 + \frac{1}{G} \, \partial_{j_t} \ell \left(h_{\theta_t}, (x,y) \right) \right) \in [0,1].$$

Fix a quantization accuracy $\alpha \in (0,1)$ and let $b = \lceil \log_2(1/\alpha) \rceil$. Then there exist Boolean functions $g_{t,1}, \ldots, g_{t,b}$ (depending on t, θ_t, j_t) and a deterministic decoder $\mathrm{Dec} : \{0,1\}^b \to [0,1]$ such that, for every (x,y),

$$\left| \operatorname{Dec} \left(g_{t,1}(x,y), \dots, g_{t,b}(x,y) \right) - \phi_t(x,y) \right| \leq \alpha.$$

Consequently, the mini-batch average of ϕ_t over B i.i.d. samples can be simulated by B calls to 1-STAT(b) at iteration t, with deterministic quantization error at most α . Choosing $\alpha = \frac{1}{2\sqrt{B}}$ ensures this quantization error is dominated by the sampling error $O(1/\sqrt{B})$.

Proof. Fix $\alpha \in (0,1)$. Define the grid

$$\mathcal{G}_b := \left\{ \frac{k}{2^b} : k = 0, 1, \dots, 2^b \right\} \subseteq [0, 1].$$

Since $b = \lceil \log_2(1/\alpha) \rceil$, the grid spacing is $2^{-b} \le \alpha$.

Define the quantizer $Q:[0,1]\to \mathcal{G}_b$ that maps $z\in[0,1]$ to the unique grid point $Q(z)\in \mathcal{G}_b$ satisfying $|Q(z)-z|\leq 2^{-b}\leq \alpha$. This map can be implemented by encoding the binary expansion of z to b bits, truncated or rounded as needed.

For each (x, y), define

$$(g_{t,1}(x,y),\ldots,g_{t,b}(x,y)):=$$
 binary representation of $Q(\phi_t(x,y)).$

By construction, each $g_{t,i}$ is a Boolean function of (x, y), and

$$Dec(g_{t,1}(x,y),\ldots,g_{t,b}(x,y)) := Q(\phi_t(x,y)).$$

Therefore

$$\left| \operatorname{Dec}(g_{t,1}(x,y), \dots, g_{t,b}(x,y)) - \phi_t(x,y) \right| \leq \alpha.$$

Now consider a mini-batch $S = \{(x_1, y_1), \dots, (x_B, y_B)\}$ of B independent draws from D. The SGD update uses the empirical average

$$\hat{v} := \frac{1}{B} \sum_{i=1}^{B} \phi_t(x_i, y_i).$$

Meanwhile, simulating with 1-STAT(b) queries, we obtain

$$\hat{v}_Q := \frac{1}{B} \sum_{i=1}^B \text{Dec}(g_{t,1}(x_i, y_i), \dots, g_{t,b}(x_i, y_i)).$$

For each i, the error $|\text{Dec}(g_{t,1}(x_i, y_i), \dots, g_{t,b}(x_i, y_i)) - \phi_t(x_i, y_i)| \leq \alpha$, hence

$$|\hat{v}_Q - \hat{v}| \le \frac{1}{B} \sum_{i=1}^B \alpha = \alpha.$$

Thus \hat{v}_Q simulates \hat{v} up to additive error α . Choosing $\alpha = 1/(2\sqrt{B})$ ensures this error is smaller than the typical sampling deviation of order $1/\sqrt{B}$, so quantization does not alter asymptotics. \Box

B.4 SIMULATING 1-STAT(B) BY VSTAT

Definition 4 (Success predicate). Let $f^* \in \mathcal{C}$ be the target and D a distribution over \mathcal{X} . Given $\epsilon \in (0, 1/2)$, an algorithm succeeds if it outputs a hypothesis $h : \mathcal{X} \to \{-1, +1\}$ with $error \leq \frac{1}{2} - \epsilon$.

Theorem 2 (Feldman et al., 2018, Thm. B.4). Let $\beta \in (0, 1]$. Suppose there exists an algorithm \mathcal{A} that uses q queries to a 1-STAT(b) oracle and, with probability at least β , succeeds in the sense of Definition 4. Then for any $\delta \in (0, 1)$ there exists an algorithm \mathcal{A}' that uses at most

$$Q = \mathcal{O}(q \, 2^b)$$
 queries to VSTAT $(\Theta(q \, 2^b/\delta^2))$

and succeeds with probability at least $\beta - \delta$.

B.5 From VSTAT Lower Bounds to SGD Iteration Lower Bounds

Proposition 2 (Lower bound for SGD). Let $\mathcal C$ be a class with $\mathrm{SQ}\text{-}\mathrm{DIM}_D(\mathcal C)=d$. Consider coordinate mini-batch SGD with batch size B run for T iterations. Fix $\epsilon\in(0,1/2)$. If the algorithm outputs a hypothesis of error at most $1/2-\epsilon$ with probability at least 2/3, then $T\geq\Omega\left(\frac{d\,\epsilon^2}{B^{3/2}}\right)$.

Proof. We prove the result by reducing any successful run of mini-batch SGD to an algorithm that makes a limited number of queries to a VSTAT oracle. This allows us to invoke standard SQ lower bounds, which force the number of SGD iterations to be large.

Step 1 (SQ lower bound at accuracy $\Theta(\epsilon)$). By the standard SQ lower bound for classes with $\mathrm{SQ\text{-}DIM}_D(\mathcal{C}) = d$ (Blum et al., 1994; see also Reyzin, 2020, Theorem 12), any learner that succeeds with error $\leq 1/2 - \epsilon$ with probability $\geq 2/3$ using a τ -tolerant SQ oracle with $\tau = \Theta(\epsilon)$ must make at least $Q^\star = \Omega(d\,\epsilon^2)$ SQ queries. Equivalently, since a single SQ query of tolerance τ can be answered by one VSTAT(t) query with $t = \Theta(1/\tau^2)$ (and vice versa), the same lower bound holds for VSTAT (t^\star) with

$$t^* = \Theta(1/\epsilon^2)$$
: any VSTAT (t^*) learner that succeeds must use $\geq Q^*$ queries. (\dagger)

Step 2 (Express one SGD step via 1-STAT and then via VSTAT). By Proposition 4, one iteration of coordinate mini-batch SGD with batch size B can be simulated by B queries to a 1-STAT(b) oracle, with $b = \lceil \log_2(2\sqrt{B}) \rceil$. Hence the full run (over T iterations) uses q = TB queries to 1-STAT(b). By Thm. 2, for any fixed $\delta \in (0,1/6)$, there is a transformation that simulates this 1-STAT(b) algorithm by an algorithm that makes $Q_0 = O(q \, 2^b) = O(TB \, 2^b)$ queries to a VSTAT (t_0) oracle (for some $t_0 = \Theta(q \, 2^b/\delta^2)$), and succeeds with probability at least $2/3 - \delta$.

Step 3 (Amplify success probability to $\geq 2/3$). Set $\delta = 1/12$. The simulated VSTAT (t_0) algorithm from Step 2 succeeds with probability $p_0 = 2/3 - \delta = 7/12$. Run r independent copies to obtain hypotheses h_1, \ldots, h_r . For each j, estimate the error $e_j := \operatorname{err}_D(h_j)$ using one VSTAT (t_{sel}) query on $h'_j(x,y) = \mathbf{1}[h_j(x) \neq y]$, with $t_{\text{sel}} = \Theta(1/\epsilon^2)$, which returns \hat{e}_j satisfying $|\hat{e}_j - e_j| \leq \epsilon/4$. Output $h_\star = \operatorname{arg\,min}_j \hat{e}_j$.

With probability $1-(1-p_0)^r$ at least one copy is ϵ -good (i.e., has $e_j \leq \frac{1}{2} - \epsilon$). On that event, the selection rule guarantees

$$e_{\star} \leq \min_{j} e_{j} + \frac{\epsilon}{2} \leq \frac{1}{2} - \epsilon + \frac{\epsilon}{2} = \frac{1}{2} - \frac{\epsilon}{2}.$$

Taking r=3 gives $1-(1-p_0)^3=1-(5/12)^3>2/3$. Thus, after a constant number of repetitions and a constant number of additional VSTAT queries (for selection), we obtain a hypothesis with error at most $\frac{1}{2}-\frac{\epsilon}{2}$ with probability >0.9. Absorbing the constant factor loss in ϵ into the big- Θ notation, this yields success probability >2/3 while multiplying the total number of VSTAT queries only by a universal constant, so $Q=\Theta(Q_0)=\Theta(TB\,2^b)$.

Step 4 (Align the oracle parameter to $t^* = \Theta(1/\epsilon^2)$). The simulation in Step 2 produces a VSTAT (t_0) oracle with parameter t_0 that may differ from t^* . We consider two cases:

Case 1: $t_0 \ge t^*$ (more accurate oracle). A VSTAT (t_0) reply is guaranteed to be closer to the true expectation than a VSTAT (t^*) reply. By post-processing (adding extra random noise), we can make each VSTAT (t_0) answer distributed exactly as a VSTAT (t^*) answer, without using additional queries. Thus any algorithm using Q queries to VSTAT (t_0) can be viewed as an algorithm using Q queries to VSTAT (t^*) .

Case 2: $t_0 < t^*$ (less accurate oracle). Suppose, for contradiction, that there exists an algorithm that succeeds with fewer than Q^* queries to $VSTAT(t_0)$. Since $VSTAT(t^*)$ is strictly more accurate, the same algorithm would also succeed with the same number of queries to $VSTAT(t^*)$ (simply by treating each $VSTAT(t^*)$ answer as a $VSTAT(t_0)$ answer). This contradicts (†).

In either case, success with at most $Q=\Theta(TB\,2^b)$ VSTAT calls would contradict (†) unless $Q\geq Q^\star=\Omega(d\,\epsilon^2)$.

Step 5 (Conclude and simplify). We have $\Theta(TB\,2^b) \geq \Omega(d\,\epsilon^2)$, i.e. $T \geq \Omega\left(\frac{d\,\epsilon^2}{B\,2^b}\right)$. Finally, with $b = \lceil \log_2(2\sqrt{B}) \rceil$ we have $2^b = \Theta(\sqrt{B})$, so $T \geq \Omega\left(\frac{d\,\epsilon^2}{B^{3/2}}\right)$, as claimed.